Driving into the Dynamics–Leveraging the Direct-Quadrature-Zero Transform for Mechanical Systems

José M. Campos-Salazar
Electronic Engineering Department
Universitat Politècnica de Catalunya
Barcelona, Spain
jose.manuel.campos@upc.edu

Abstract—**This research offers a thorough analysis of the dynamic behavior of 1-, 2-, and 3-DoF mechanical systems under a sinusoidal force, examining both mechanical and dq coordinates. By utilizing standardized initial conditions, the 1-DoF system displays fascinating oscillatory patterns with dual frequency components, highlighting the significance of low damping. The adaptation to dq coordinates simplifies the analysis and highlights the system's nuanced behavior. In contrast, the 2-degree-of-freedom system exhibits intricate interactions, oscillation phenomena, and multiple frequency components in mechanical coordinates. The contribution of masses that do not experience external forces in dq coordinates is minimal. On the other hand, the 3-degree-of-freedom system shows diverse interactions and frequency components that are different from the dq transformations. The observed dynamics not only enhance comprehension of these systems but also provide valuable insights for refining analytical approaches in the analysis of dynamic systems. This study sets the stage for future investigations and urges the development of streamlined analytical frameworks for a more focused exploration of externally influenced variables in dynamic mechanical systems.**

Keywords—Dynamic analysis, dq coordinates, multi-DOF systems, mechanical system dynamics

I. INTRODUCTION

Vibration analysis, a core aspect of mechanical engineering, is dedicated to understanding the complex behavior of mechanical systems subjected to oscillations or vibrations due to external forces or displacements [1]. This field has deep significance in various sectors, including industry [2]–[6], automation [7]–[10], and aerospace [11], [12], as it provides a mechanism for designing, controlling, optimizing, and maintaining the performance, safety, and reliability of mechanical systems.

For instance, the paper in [2] emphasizes the need to address vibrational complexity in dynamic mechanical systems. It highlights the challenges in dynamic vibration analysis due to factors such as frequency and damping. This article takes a look at methods such as modal analysis, Fourier transform, wavelet analysis, and computational simulation to overcome these hurdles and gain insight into mechanical vibrations. This article confirms the central role of vibration concepts in the design, operation, and maintenance of mechanical systems, providing indispensable knowledge for engineers and operators.

In addition, a comprehensive review in [3] addresses vibration analysis techniques for diagnosing rolling bearing failures in machinery, emphasizing the importance of accurate fault diagnosis to ensure the performance and reliability of industrial machinery. This review navigates the complexities of bearing fault identification due to the variety of operating conditions and fault types. The study explains various vibration analysis methods, including time-domain, frequency-domain, and time-frequency-domain techniques. By carefully examining these methods, the review underscores their importance in the early detection of bearing failures, thereby enabling predictive maintenance and reducing industrial downtime.

In process plants, an article discussed in [4] emphasizes the pivotal role of careful machine management, which is essential for smooth plant operation and productivity. The article addresses the challenges of mechanical failures that can result in costly shutdowns. By exploring pragmatic machine management strategies such as condition monitoring and preventive maintenance, this article underscores the importance of predictive techniques such as vibration analysis in identifying and addressing mechanical problems before they arise. The study introduces the diverse methods of dynamic vibration analysis and illustrates their effectiveness in diagnosing component failures and irregularities.

Following this line, the book in [5] deals with the basic concepts and techniques of vibration analysis for single-degree-of-freedom mechanical systems. This chapter emphasizes the importance of understanding and analyzing the dynamic behavior of these systems as a basis for more complex mechanical structures. The book explains the principles of vibration analysis and emphasizes its importance in characterizing the vibrational response of systems to external forces or disturbances. It addresses the challenge of prediction and management of mechanical vibrations that can lead to performance degradation and potential failure. It rigorously evaluates methods for analyzing these systems, ranging from dynamic response to harmonic excitation, transient response, and resonance phenomena, emphasizing the centrality of vibration analysis in engineering design and maintenance.

In the automotive context, a comprehensive study in [6] examines active vibration control techniques and shows their importance in suppressing the negative effects of vibration on vehicles, from passenger discomfort to performance degradation. The article examines advanced methods for controlling and minimizing vibration, emphasizing the need to integrate cutting-edge technologies. It explores the challenging process of achieving optimal vibration control in dynamic

automotive environments and outlines various techniques and strategies for accomplishing this task.

In this automotive field, [7] presents an experimental analysis that highlights the symbiotic relationship between maintenance and mechanical vibration in the automotive sector. The article emphasizes the effects of inadequate maintenance, leading to escalated vibrations and potential mechanical failures. It addresses the challenges of dynamic vibration analysis under varying conditions and vehicle systems. The article analyzes methods such as sensor-based data acquisition and signal processing techniques, including fast Fourier transform, to analyze and control vibration. The importance of maintenance practices in mitigating vibration and improving vehicle performance and safety is highlighted.

The field of automotive mechanical transmission systems is highlighted in [8], emphasizing their critical role in minimizing torsional vibration. Addressing torsional vibration emerges as a requirement for the optimal function and lifetime of transmission systems. The challenges associated with torsional vibration analysis and mitigation, particularly in complex automotive transmission systems, are explored. The study examines techniques such as torsional dampers and optimization of gear engagement strategies to suppress vibration, emphasizing the importance of well-designed transmission systems for improved vehicle performance and reduced friction.

The perspective is expanded in [9] with a study that provides comprehensive analysis and comparison methods for automotive vibration testing. The article highlights the key role of vibration testing in evaluating the reliability and performance of automotive components and systems. It addresses the challenges inherent in performing and analyzing vibration tests, especially in the complex automotive environment. This work covers a range of methods used to analyze and compare vibration test results, including frequency domain analysis, time domain analysis, and statistical approaches. This in-depth analysis extracts invaluable insights from vibration tests, leading to optimized vehicle design and performance, ensuring the safety, comfort, and overall excellence of automotive systems.

Moving to the scope of noise and vibration management in the automotive sector, the work in [10] develops. This article highlights the importance of mitigating the detrimental effects of noise and vibration on vehicle performance, passenger comfort, and customer satisfaction. The paper recognizes the energy of the industry in addressing this challenge with strategies and technologies involving advanced materials, structural optimization, and active noise and vibration control systems. The fusion of engineering, design, and acoustics emerges as a primary approach to reducing the noise and vibration spectrum, resulting in an enhanced vehicle experience. This industry commitment resonates with the constant search for automotive excellence through noise and vibration management.

In aerospace, vibration analysis of mechanical systems plays a critical role in failure prevention [11]. The mechanical simulation analysis of high-reliability aerospace electronic equipment described in [11] underscores the criticality of aerospace dynamic vibration analysis, especially for high-reliability electronic components. It highlights the challenging path through aerospace dynamic vibration, dealing with severe environments and complex interactions. The article explores finite element analysis, computer simulation, and experimental testing that are critical to predicting and mitigating the effects of vibration on equipment. These methods embed reliability, safety, and optimal performance, symbolizing the aerospace industry's commitment to rigorous vibration analysis practices.

In discussing aerospace vibration, [12] focuses on flexible structures, describing their susceptibility to vibration and how that vibration can affect safety and performance. The article turns its attention to innovative solutions such as active disturbance rejection control, which is well suited to suppressing vibrations through active disturbance suppression. Frequency-domain analysis methods are injected into this approach to enhance the understanding and mitigation of vibration-induced problems. This paper highlights the aerospace industry's application of innovative solutions to managing vibration in complex, flexible aircraft systems.

As systems increase in complexity and degrees of freedom, vibrational analysis continues to rise [1]. However, these methods face difficult challenges that complicate analysis efforts [1]. For instance, [13] addresses mechanical system dynamics involving lateral vibrations in transportation applications. The challenges include analyzing and predicting the lateral vibration responses of these systems, a challenging task. These systems involve complex structural interactions, varying loads, and forces, all in an effort to maintain structural integrity and safety in dynamic transportation environments. The precision of dynamic analysis rises as the basis for designing transportation systems to withstand vibrational attack.

Mechanical systems susceptible to failure modes due to vibration and fatigue are involved in the complex field of system reliability [14]. The study in [14] deals with predicting system reliability in the presence of dynamic forces that culminate in failures due to fatigue and vibration. The complicated mesh of abrasive processes, vibration dynamics, and their fatal interactions show a complex duality. Appropriate modeling of the interaction of vibration and fatigue emerges as a critical compass that enhances insight into failure mechanisms and system reliability. The goal of this effort - to design robust systems that can withstand the violent forces of fatigue and vibration - resonates as the ultimate search for improved reliability.

The book [15] presents an overview of the current challenges in modeling vibrational fatigue and fracture of structures. It also explores the difficult environment of modeling vibrational fatigue and fracture behavior in various structures. It emphasizes the complexities and challenges associated with accurately predicting the fatigue life and fracture behavior of structures under dynamic loading conditions. The study highlights the diverse nature of vibrational fatigue, which includes factors such as material properties, loading conditions, environmental effects, and the

intricate interplay between vibrational dynamics and fatigue behavior. The article highlights the difficulties in developing comprehensive and accurate computational models that capture the intricate details of vibrational fatigue and fracture phenomena. It also highlights the need to consider the synergistic effects of multiple influencing factors, such as resonance, stress concentration, and environmental conditions, when modeling and predicting vibrational fatigue and fracture of structures. By providing a comprehensive review of the current challenges, methodologies, and advances in the field, the article serves as a valuable resource for researchers and practitioners working toward more accurate and reliable models for predicting the vibrational fatigue and fracture behavior of structures.

The methods used to analyze vibrating systems are varied. In [16], an in-depth exploration of various vibration analysis methods applied to rotating machinery for predictive maintenance is provided. Traditional techniques such as time and frequency domain analysis are discussed along with advanced methods such as time-frequency domain analysis and AI-based approaches including support vector machines and neural networks. The article emphasizes the importance of these techniques in achieving early fault detection and ensuring the reliability of mechanical systems in various industries.

A review of prediction methods for transient vibration and sound radiation of plates is reported in [17]. This article presents a comprehensive review of the prediction methods for transient vibration and sound radiation of plates. It covers traditional techniques such as finite element analysis and boundary element methods, as well as more recent developments such as wave-based methods and hybrid approaches. The article highlights the importance of these methods in analyzing the dynamic behavior and sound radiation of plate structures in various applications, contributing to improved design and performance optimization.

The article [18] delves into the innovative approach of utilizing non-traditional dynamic vibration absorbers to mitigate vibrations in damped linear structures. It underscores the significance of vibration control in enhancing the performance and longevity of mechanical systems. The article explores various methods and strategies to design and implement dynamic vibration absorbers, deviating from conventional approaches. By leveraging non-traditional absorbers, which could include magneto-rheological dampers, the study aims to optimize vibration reduction in real-world applications. This research highlights the evolution of vibration control techniques and their potential to revolutionize the field of structural dynamics and mechanical engineering.

In [19] provides a comprehensive exploration of the field of vibration analysis in machine monitoring and diagnostics. It highlights the central role of vibration analysis in various industries, including manufacturing, automotive, and aerospace, in ensuring the reliable operation of complex mechanical systems. The study examines the challenges inherent in the analysis of dynamic mechanical vibration, ranging from the complexity of signal processing to the need for expertise in fault detection. Traditional methods used in this context are examined in detail, including time, frequency, and time-frequency domain techniques. In addition, the article highlights the emerging integration of artificial intelligence (AI) techniques, such as support vector machines, neural networks, fuzzy logic, and genetic algorithms, to improve the accuracy and automation of fault diagnosis. The research underscores the importance of adapting vibration analysis to the evolving environment of smart machines and digital twins while recognizing the need to address the challenges associated with non-Gaussian noise and the generalization of AI models. Through a comprehensive review of influential articles, this study contributes to the advancement of vibration analysis for machine health monitoring and diagnosis.

A modal analysis of the Karun-4 concrete arch dam is presented in [20]. In this study the authors use a finite element model of the dam-reservoir-foundation system and compare the results with the ambient vibration tests. They study the effects of reservoir water level, foundation rock mass, and earthquake excitation on the natural frequencies and mode shapes of the dam. They find that the reservoir water level has a significant effect, the foundation rock mass has a minor effect, and the earthquake excitation has a negligible effect on the modal properties of the dam. They conclude that their model is useful for evaluating.

Finally, the article in [21] presents modal analysis, which is a technique for studying the dynamic properties of structures and systems. The authors review the test procedure and system identification principles of modal analysis. They also discuss the main practical problems and new trends in modal analysis. They illustrate them with case studies. The article is useful for researchers and engineers interested in modal analysis.

From the literature review developed in the previous paragraphs, it can be seen that the methods used for vibrational analysis are based on the frequency domain, time domain, with the use of neural networks, artificial intelligence and modal dynamics. However, using these methods, the vibrational nature of the variables (usually of the sinusoidal type) dynamics of the systems remain unchanged. When applying a linear control system, it becomes very difficult to design it, since regulating variables of sinusoidal nature, introduces different operating points as the sinusoidal variable progresses, even in steady state [22]–[24].

An approach that allows to solve this drawback is to apply a linear transformation of the tensor type that rotates the reference frame of a three-element vector or a three-by-three element matrix in an effort to simplify analysis [25]. This transformation is called direct-quadrature-zero transformation (dq0) [25].

It is interesting to see that there are no reported works that cover a vibrational analysis of a mechanical system using dq0. Therefore, this article presents a study that analyzes a mechanical dynamic system with vibrations of one, two, and three degrees of freedom using the dq0. The dynamic models in the natural mechanical frame and the corresponding model in the rotating dq0 frame are obtained.

The paper is organized as follows; section II presents and examines the Park and Clarke linear transforms, followed by the mathematical analysis of the dqo transform applied to

vibrational mechanical systems in section III. Section IV analyzes the energy equations relating to the vibrational systems proposed in this study. The state variable expressions for the vibrational models analyzed in this study are derived and analyzed in Section V. The simulation results and conclusions are presented in sections VI and VII, respectively.

II. PARK AND CLARKE TRANSFORMATION ANALYSIS

The Clarke ($\alpha\beta0$) and dq0 transformations play a crucial role in the field of electricity and power electronics, and are widely recognized for their versatile applications [26]–[30]. These transformations are fundamental methods for converting three-phase quantities, such as voltages or currents, from the conventional abc reference frame to the dq0 reference frame. In the abc reference frame, each phase is represented as a sinusoidal function with a 120° phase shift, which is the natural coordinate system for three-phase systems. In contrast, the dq0 reference frame is a rotating coordinate system that is carefully aligned with either the magnetic flux of a machine or the voltage vector of an inverter. Within the dq0 reference frame, two orthogonal axes, known as the d-axis and the q-axis, correspond exactly to the direct and quadrature components of the three-phase magnitude. In addition, the dq0 reference frame includes a zero-sequence component that effectively represents the common-mode or neutral aspect of the three-phase magnitude [25].

These transformations, $\alpha\beta0$ and dq0, are intrinsically linked by a rotation matrix. The $\alpha\beta0$ transformation transforms abc quantities into stationary $\alpha\beta0$ quantities that are aligned with the stationary axes of the machine or drive. Conversely, the dq0 transformation takes these stationary $\alpha\beta0$ quantities and transforms them into dynamic dq0 quantities that are precisely aligned with the rotating axes of the machine or drive. The exact angle of rotation in dq0 depends on the angular position or speed of the machine or drive [25].

In addition, $\alpha\beta0$ and dq0 offer a variety of advantages in the three-phase domain. They simplify the mathematical representation of these systems by reducing them to single-phase or two-phase models, which greatly reduces computational complexity. In addition, these transformations decouple the active and reactive power components, effectively splitting them into d and q components, allowing a deeper understanding and control of power distribution. In addition, they enable the implementation of vector control techniques in machines and inverters, providing direct control over critical parameters such as torque, flux, voltage, and current, ultimately improving system performance and efficiency [25].

In essence, the $\alpha\beta0$ and dq0 transformations provide essential bridges between the conventional abc and dq0 reference frames, making three-phase electrical systems more understandable and controllable. Their solid mathematical foundations and versatile applications are central to the fields of power electronics and electrical engineering.

A. Derivation of the Clarke Transformation Matrix

The $\alpha\beta0$ transformation, a powerful tool in electrical engineering, functions as an essential bridge between vectors in the conventional abc reference frame and the $\alpha\beta0$ reference frame. Its primary strength lies in its remarkable ability to disentangle the components of an abc-referenced vector by emphasizing the common element shared by all three vector components - in particular, it emphasizes the common-mode component, often referred to as the Z component [25], [31]. This transformation is supported by a number of features: it maintains power invariance, adheres to right-handed coordinate system conventions, and follows uniform scaling principles [25], [31]. The core of this transformation is represented by the power-invariant, right-handed, uniformly scaled Clarke transform matrix defined as follows

$$\mathbf{K_C} = \sqrt{\frac{2}{3}} \cdot \begin{bmatrix} 1 & -\frac{1}{2} & -\frac{1}{2} \\ 0 & \frac{\sqrt{3}}{2} & -\frac{\sqrt{3}}{2} \\ \frac{1}{\sqrt{2}} & \frac{1}{\sqrt{2}} & \frac{1}{\sqrt{2}} \end{bmatrix} \tag{1}$$

To convert an abc-referenced system represented as a time-domain column vector ($\mathbf{m_{abc}}(t)$) into a corresponding time-domain column vector in the $\alpha\beta0$ reference frame ($\mathbf{m_{\alpha\beta0}}(t)$), the abc vector must undergo a pre-multiplication process with the transformation matrix $\mathbf{K_C}$, as shown in follows

$$\mathbf{m_{\alpha\beta0}}(t) = \mathbf{K_c} \cdot \mathbf{m_{abc}}(t) \tag{2}$$

On the other hand, to return to the abc frame (i.e., $\mathbf{m_{\alpha\beta0}}(t)$), both sides of equation (2) must be pre-multiplied by the inverse of $\mathbf{K_C}$, resulting in as follows

$$\mathbf{m_{abc}}(t) = \mathbf{K_c}^{-1} \cdot \mathbf{m_{\alpha\beta0}}(t) \tag{3}$$

In essence, the $\alpha\beta0$ transformation is a fundamental tool in electrical engineering that simplifies the manipulation of vectors between the abc and $\alpha\beta0$ reference frames while preserving important mathematical properties and conventions.

B. Derivation of the Park Transformation Matrix

The dq0 transformation plays a central role in the conversion of vectors originating in the $\alpha\beta0$ reference frame to the dq0 reference frame, and has considerable utility in various applications [25], [31]. Its primary function is to facilitate a controlled realignment of a vector's reference frame, a process often referred to as "soft rotation," which occurs at a user-defined frequency. One of its critical features is the precise manipulation of a signal's frequency spectrum. This manipulation allows the user-specified frequency to appear as a dc frequency while simultaneously inverting the original dc frequency to match the specified frequency. This transformation effectively recalibrates the frequency alignment, making it a fundamental tool in numerous engineering and control contexts [25], [31].

Mathematically, the dq0 transformation is expressed in its matrix representation, defined in (4). Here, $\theta(t)$ represents the instantaneous angle corresponding to an arbitrary angular

$$K_P = \begin{bmatrix} \cos\theta(t) & \sin\theta(t) & 0 \\ -\sin\theta(t) & \cos\theta(t) & 0 \\ 0 & 0 & 1 \end{bmatrix} \qquad (4)$$

frequency ($\omega(t)$) [25], [31]. To convert a time-domain column vector in the $\alpha\beta0$ reference frame, denoted $\mathbf{m}_{\alpha\beta0}(t)$, into a new time-domain column vector in the dq0 reference frame, $\mathbf{m}_{dq0}(t)$, the following expression must be satisfied

$$\mathbf{m}_{dq0}(t) = K_P \cdot \mathbf{m}_{\alpha\beta0}(t) \qquad (5)$$

Similarly, to return to the $\alpha\beta0$ frame, the inverse transformation is required, given by

$$\mathbf{m}_{\alpha\beta0}(t) = K_P^{-1} \cdot \mathbf{m}_{dq0}(t) \qquad (6)$$

Extending the previous information, it is possible to derive the transformation matrix for directly transforming a time-domain column vector from the abc reference frame into a new time-domain column vector in the dq0 reference frame. This matrix is derived as $K_{CP} = K_C \cdot K_P$, resulting in

$$K_{CP} = \sqrt{\frac{2}{3}} \cdot \begin{bmatrix} \cos\theta(t) & \cos\left(\theta(t) - \frac{2\cdot\pi}{3}\right) \\ -\sin\theta(t) & -\sin\left(\theta(t) - \frac{2\cdot\pi}{3}\right) \\ \frac{\sqrt{2}}{2} & \frac{\sqrt{2}}{2} \end{bmatrix}$$
$$\begin{matrix} \cos\left(\theta(t) + \frac{2\cdot\pi}{3}\right) \\ -\sin\left(\theta(t) + \frac{2\cdot\pi}{3}\right) \\ \frac{\sqrt{2}}{2} \end{matrix} \qquad (7)$$

$$K_{CP}^{-1} = \sqrt{\frac{2}{3}} \cdot \begin{bmatrix} \cos\theta(t) \\ \cos\left(\theta(t) - \frac{2\cdot\pi}{3}\right) \\ \cos\left(\theta(t) + \frac{2\cdot\pi}{3}\right) \end{bmatrix}$$
$$\begin{matrix} -\sin\theta(t) & \frac{\sqrt{2}}{2} \\ -\sin\left(\theta(t) - \frac{2\cdot\pi}{3}\right) & \frac{\sqrt{2}}{2} \\ -\sin\left(\theta(t) + \frac{2\cdot\pi}{3}\right) & \frac{\sqrt{2}}{2} \end{matrix} \qquad (8)$$

$$\mathbf{m}_{dq0}(t) = K_{CP} \cdot \mathbf{m}_{abc}(t) \qquad (9)$$
$$\mathbf{m}_{abc}(t) = K_{CP}^{-1} \cdot \mathbf{m}_{dq0}(t) \qquad (10)$$

Then, with a corresponding inverse transform defined in (8). For the direct conversion of a time column vector referenced in abc ($\mathbf{m}_{abc}(t)$) into a time column vector in the dq0 frame ($\mathbf{m}_{dq0}(t)$), equation (9) is used. Conversely, for a return to the abc frame, equation (10) is used.

In a geometric context, the dq0 transformation, much like the $\alpha\beta0$ transformation, is rooted in the principles of dot products and vector projections [25], [31]. To illustrate this concept, consider an $\alpha\beta$ reference frame and a dq reference frame displayed simultaneously (see Fig. 1). The 0 coordinate is intentionally omitted in both reference frames for clarity. In this scenario, a vector is displayed in the $\alpha\beta$ frame, $\mathbf{m}_{\alpha\beta}(t)$. Note that the dq frame is shifted by $\theta(t)$ degrees from the $\alpha\beta$ reference frame.

The Cartesian representation of $\mathbf{m}_{\alpha\beta}(t)$ in terms of the $\alpha\beta$ frame is defined as

$$\mathbf{m}_{\alpha\beta}(t) = \mathbf{m}_\alpha(t) \cdot \hat{\mathbf{u}}_\alpha + \mathbf{m}_\beta(t) \cdot \hat{\mathbf{u}}_\beta \qquad (11)$$

Here, $\hat{\mathbf{u}}_\alpha$ and $\hat{\mathbf{u}}_\beta$ denote the unit basis vectors corresponding to the α and β components of the $\alpha\beta$ reference frame. The angle $\theta(t)$ represents the orientation between $\hat{\mathbf{u}}_\alpha$ and $\hat{\mathbf{u}}_d$ [25], [31]. Referring to Fig. 1, the unitary vectors for the d and q components with respect to the α and β components can be defined as follows

$$\begin{cases} \hat{\mathbf{u}}_d = \cos(\theta(t)) \cdot \hat{\mathbf{u}}_\alpha + \sin(\theta(t)) \cdot \hat{\mathbf{u}}_\beta \\ \hat{\mathbf{u}}_q = -\sin(\theta(t)) \cdot \hat{\mathbf{u}}_\alpha + \cos(\theta(t)) \cdot \hat{\mathbf{u}}_\beta \end{cases} \qquad (12)$$

The projection of the vector $\mathbf{m}_{\alpha\beta}(t)$ onto the unit vectors of the d and q frames, i.e., $\hat{\mathbf{u}}_d$ and $\hat{\mathbf{u}}_q$, can be understood through the concept of the dot product where $\mathbf{m}_d(t)$ represents the projection of $\mathbf{m}_{\alpha\beta}(t)$ onto the $\hat{\mathbf{u}}_d$ axis, and $\mathbf{m}_q(t)$ represents the projection onto the $\hat{\mathbf{u}}_q$ axis as can be seen as follows

$$\begin{cases} \mathbf{m}_d(t) = \hat{\mathbf{u}}_d \cdot \mathbf{m}_{\alpha\beta}(t) = \\ = \cos(\theta(t)) \cdot \mathbf{m}_\alpha(t) + \sin(\theta(t)) \cdot \mathbf{m}_\beta(t) \\ \mathbf{m}_q(t) = \hat{\mathbf{u}}_q \cdot \mathbf{m}_{\alpha\beta}(t) = \\ = -\sin(\theta(t)) \cdot \mathbf{m}_\alpha(t) + \cos(\theta(t)) \cdot \mathbf{m}_\beta(t) \end{cases} \qquad (13)$$

Together, these projected components, $\mathbf{m}_d(t)$ and $\mathbf{m}_q(t)$, constitute the new vector, $\mathbf{m}_{dq}(t)$, within the dq reference frame [25], [31]. It is important to note that the positive angle $\theta(t)$ corresponds to a counter-clockwise rotation of the vector as it transitions to the new dq reference frame. This implies that the angle of the vector relative to the new reference frame is smaller than its angle within the old reference frame (i.e., the $\alpha\beta$ reference frame). This difference arises from the fact that it is the reference frame itself that has undergone a forward rotation,
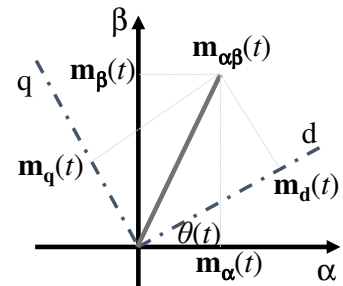

Fig. 1. Geometric representation of an arbitrary vector $\mathbf{m}_{\alpha\beta}(t)$ in reference frames $\alpha\beta$ and dq. In addition, the vector components of the vector in its two reference frames are included.

not the vector. In essence, a forward rotation of the reference frame is equivalent to a negative rotation of the vector. In scenarios where the original reference frame experiences a forward rotation, such as in three-phase electrical systems, the resulting dq vector ($\mathbf{m_{dq}}(t)$) essentially maintains its position without further rotation [25], [31]. In this analysis, two-component column vectors, ($\mathbf{m_\alpha}(t)$, $\mathbf{m_\beta}(t)$) and ($\mathbf{m_d}(t)$, $\mathbf{m_q}(t)$), for the αβ and dq reference frames, respectively. Thus, a 2x2 matrix containing these column vectors is defined as

$$\mathbf{K_P} = \begin{bmatrix} \cos\theta(t) & \sin\theta(t) \\ -\sin\theta(t) & \cos\theta(t) \end{bmatrix} \quad (14)$$

This matrix establishes the relationship expressed as $\mathbf{m_{dq}}(t) = \mathbf{K_P} \cdot \mathbf{m_{\alpha\beta}}(t)$.

In cases where a single vector quantity consists of a single component, such as $\mathbf{m_a}(t)$, a direct application of the transformation defined in (9) may not be straightforward. However, the transformation associated with (14) can be used, as explained in [32]. The core idea is to apply the Clarke transformation to the vector $\mathbf{m_a}(t)$, but in a simplified way. Specifically, the transformation is defined as follows

$$\begin{cases} \mathbf{m_\alpha}(t) = \mathbf{m_a}(t) \\ \mathbf{m_\beta}(t) = \mathbf{m_a}\left(t - \dfrac{\pi}{2}\right) \end{cases} \quad (15)$$

where $\mathbf{m_\alpha}(t)$ and $\mathbf{m_\beta}(t)$ denote the components of $\mathbf{m_a}(t)$ in the αβ frame. This transformation retains the original component as $\mathbf{m_\alpha}(t)$, while the β component, $\mathbf{m_\beta}(t)$, corresponds to the original vector shifted by 90 degrees. Consequently, the vector $\mathbf{m_{\alpha\beta}}(t)=[\mathbf{m_\alpha}(t), \mathbf{m_\beta}(t)]^T$ can be converted into $\mathbf{m_{dq}}(t)$ by applying (14) [25], [31].

III. APPLICATION OF THE PARK TRANSFORMS INTO A DYNAMIC VIBRATIONAL MECHANICAL SYSTEM

This section discusses the mathematical analysis of the dq0 transformation method within vibrational mechanical-dynamical systems. These systems include one-degree-of-freedom (1-DoF), two-degree-of-freedom (2-DoF), and three-degree-of-freedom (3-DoF) configurations, as shown in Fig. 2(a), (b), and (c) respectively.

Each of the models shown in Fig. 2 has different arrangements characterized by specific parameters, including mass (m_i), stiffness (k_i), and damping (b_i), where $i \in \{1, 2, 3\}$. It is important to note that these masses (m_i) are treated as rigid and inelastic bodies, fixed to immovable structures [33].

In Fig. 2(a), a system with a single mass, denoted m_1, is connected to a wall through a spring element (k_1) and a damper (b_1).

Fig. 2(b) shows a more complex system with two masses, m_1 and m_2. In this configuration, m_1 is connected to the wall through elements k_1 and b_1, while it is also connected to m_2 through elements k_2 and b_2.

Finally, Fig. 2(c) shows a three-mass system with m_1, m_2, and m_3. Similar to the previous configurations, m_1 is connected to the wall by elements k_1 and b_1. In addition, m_1 and m_3 are coupled to m_2 by elements (k_2, b_2) and (k_3, b_3), respectively. The units for m_i, k_i, and b_i (where $i \in \{1, 2, 3\}$) are Newton (N), Newton per meter (N/m), and Newton seconds per meter (N-s/m), respectively.

In summary, the dynamic variables for the systems shown in Fig. 2 are the external force $f_1(t)$ and the positional displacements $x_i(t)$, where $i \in \{1, 2, 3\}$. Specifically, $f_1(t) = F \cdot \sin(\omega \cdot t)$, where F is the amplitude and ω is the angular frequency of the excitation force.

A. Analysis of a Mechanical Vibrational Dynamical System of One-Degree-of-Freedom

In this section, the analysis focuses on a 1-DoF vibrational mechanical system, as shown in Fig. 2(a). The aim is to derive the energy equations of the system and to establish the fundamental form of the Lagrangian equation for the generalized coordinates ($p_i(t)$) [34], which is applied to this non-conservative system. This analysis yields the dynamical equation of motion for the system in Fig. 2(a). Specifically, it provides expressions for the kinetic ($KE(t)$), potential ($PE(t)$), and dissipation ($DE(t)$) energies of the system as follows

$$\begin{cases} KE(t) = \dfrac{1}{2} \cdot m_1 \cdot \dot{x}_1(t)^2 \\ PE(t) = \dfrac{1}{2} \cdot k_{eq_1} \cdot x_1(t)^2 \\ DE(t) = \dfrac{1}{2} \cdot b_{eq_1} \cdot \dot{x}_1(t)^2 \end{cases} \quad (16)$$

Here, $b_{eq1} = b_1 + b_2$ and $k_{eq1} = k_1 + k_2$. The Lagrangian equation for $p_i(t)$ is given by

$$\frac{d}{dt}\frac{\partial KE(t)}{\partial \dot{p}_i(t)} - \frac{\partial KE(t)}{\partial p_i(t)} + \frac{\partial PE(t)}{\partial p_i(t)} + \frac{\partial DE(t)}{\partial \dot{p}_i(t)} = \Psi_i(t) \quad (17)$$

where $\psi_1(t)$ is a generalized external force acting on the system and, in this case, $\psi_1(t) = f_1(t)$.

It's important to note that $p_1(t) = x_1(t)$. By developing the energy expressions according to the Lagrange equation and then algebraically manipulating them, the dynamic equation of motion is obtained in the state-space representation

$$\begin{cases} \dfrac{d\mathbf{q}(t)}{dt} = \mathbf{A} \cdot \mathbf{q}(t) + \mathbf{B} \cdot u(t) \\ \mathbf{y}(t) = \mathbf{C} \cdot \mathbf{q}(t) + \mathbf{D} \cdot u(t) \end{cases} \quad (18)$$

Here, $\mathbf{q}(t)$ and $\mathbf{y}(t)$ are the state and output vectors, while $u(t)$ represents the scalar input to the system. Specifically, $\mathbf{q}(t) = [q_1(t), q_2(t)]^T$, where $q_1(t) = x_1(t)$ and $q_2(t) = dx_1(t)/dt$, and $u(t) = f_1(t)$. Symbolically, $\{\mathbf{q}(t), \mathbf{y}(t)\} \in \{\mathbb{R}^2\}$. The matrices $\mathbf{A}$, $\mathbf{B}$ are defined as follows

$$\mathbf{A} = \begin{bmatrix} 0 & 1 \\ -\dfrac{k_{eq1}}{m_1} & -\dfrac{b_{eq1}}{m_1} \end{bmatrix} \quad \mathbf{B} = \begin{bmatrix} 0 \\ \dfrac{1}{m_1} \end{bmatrix} \quad (19)$$
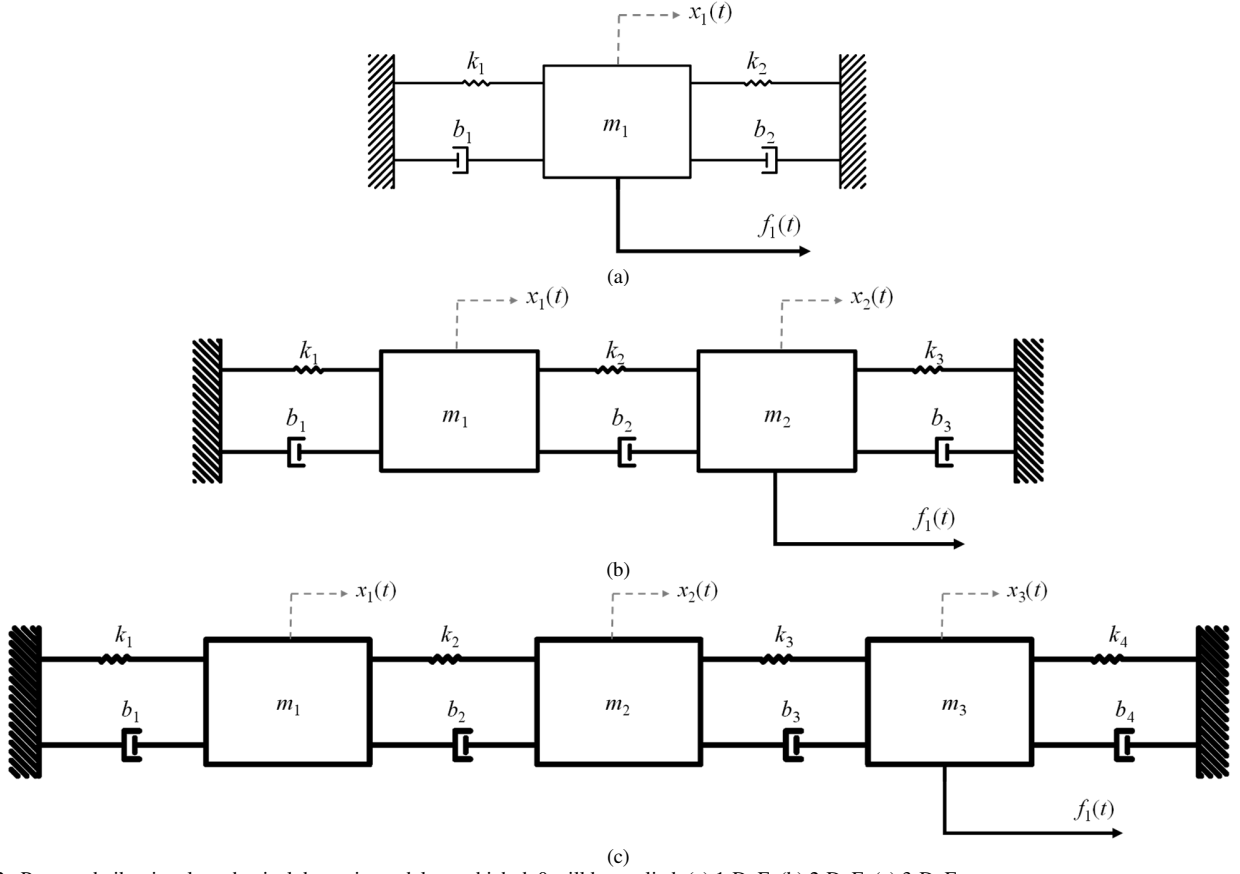
Fig. 2. Proposed vibrational mechanical dynamic models to which dq0 will be applied. (a) 1-DoF. (b) 2-DoF. (c) 3-DoF

and the two matrices $\mathbf{C}$ and $\mathbf{D}$ are the identity matrix ($\mathbf{I}$) and the zero matrix ($\mathbf{0}$), respectively. In this context, $\mathbf{A}$ is the state matrix, $\mathbf{B}$ is the input matrix, $\mathbf{C}$ is the output matrix, and $\mathbf{D}$ is the direct transmission matrix. Symbolically, $\{\mathbf{A}, \mathbf{C}\} \in \mathcal{M}_{2x2}$ and $\{\mathbf{B}, \mathbf{D}\} \in \mathcal{M}_{2x1}$.

To apply the dq0 transformation to this model, it is necessary to convert it to $\alpha\beta$ coordinates. This conversion is achieved by introducing the following relations

$$
\begin{cases}
q_{1\alpha}(t) = q_1(t) \\
q_{1\beta}(t) = q_1\left(t - \dfrac{\pi}{2}\right) \\
q_{2\alpha}(t) = q_2(t) \\
q_{2\beta}(t) = q_2\left(t - \dfrac{\pi}{2}\right) \\
u_\alpha(t) = u(t) \\
u_\beta(t) = u\left(t - \dfrac{\pi}{2}\right)
\end{cases}
\tag{20}
$$

inspired by (15). These relations yield three orthogonal vectors: $\mathbf{q}_{\alpha\beta}(t) = [q_{1\alpha}(t), q_{1\beta}(t), q_{2\alpha}(t), q_{2\beta}(t)]^T$, $\mathbf{y}_{\alpha\beta}(t) = \mathbf{q}_{\alpha\beta}(t)$, and $\mathbf{u}_{\alpha\beta}(t) = [f_{1\alpha}(t), f_{1\beta}(t)]^T$. Symbolically, $\{q_{\alpha\beta}(t), y_{\alpha\beta}(t)\} \in \{\mathbb{R}^4\}$ and $\mathbf{u}_{\alpha\beta}(t) \in \{\mathbb{R}^2\}$. Substituting these relations into the previous dynamical equation, a vector and matrix equation is derived that represents the dynamics of the 1-DoF system in $\alpha\beta$ coordinates, defined in (21). The matrices $\mathbf{A}_{\alpha\beta}$ and $\mathbf{B}_{\alpha\beta}$ are defined similarly to $\mathbf{A}$, $\mathbf{B}$

$$
\begin{cases}
\dfrac{d\mathbf{q}_{\alpha\beta}(t)}{dt} = \mathbf{A}_{\alpha\beta} \cdot \mathbf{q}_{\alpha\beta}(t) + \mathbf{B}_{\alpha\beta} \cdot \mathbf{u}_{\alpha\beta}(t) \\
\mathbf{y}_{\alpha\beta}(t) = \mathbf{C}_{\alpha\beta} \cdot \mathbf{q}_{\alpha\beta}(t) + \mathbf{D}_{\alpha\beta} \cdot \mathbf{u}_{\alpha\beta}(t)
\end{cases}
\tag{21}
$$

but in $\alpha\beta$ coordinates in

$$
\mathbf{A}_{\alpha\beta} = \begin{bmatrix}
0 & 0 & 1 & 0 \\
0 & 0 & 0 & 1 \\
-\dfrac{k_{eq_1}}{m_1} & 0 & -\dfrac{b_{eq_1}}{m_1} & 0 \\
0 & -\dfrac{k_{eq_1}}{m_1} & 0 & -\dfrac{b_{eq_1}}{m_1}
\end{bmatrix}
$$

$$
\mathbf{B}_{\alpha\beta} = \begin{bmatrix}
0 & 0 \\
0 & 0 \\
\dfrac{1}{m_1} & 0 \\
0 & \dfrac{1}{m_1}
\end{bmatrix}
\tag{22}
$$

and the matrices $\mathbf{C}_{\alpha\beta}$ and $\mathbf{D}_{\alpha\beta}$ are the identity and zero, respectively. These matrices can be expressed as $\{\mathbf{A}_{\alpha\beta}, \mathbf{C}_{\alpha\beta}\} \in \mathcal{M}_{4x4}$ and $\{\mathbf{B}_{\alpha\beta}, \mathbf{D}_{\alpha\beta}\} \in \mathcal{M}_{4x2}$.

Now, to obtain the dynamic equations of the system in dq coordinates, the transformation matrix $\mathbf{K}_\mathbf{p}$ defined in (14) is applied to the model in $\alpha\beta$ coordinates. This results in the

model of the system in dq coordinates is shown as follows

$$\begin{cases} \dfrac{d\mathbf{q_{dq}}(t)}{dt} = \mathbf{A_{dq}} \cdot \mathbf{q_{dq}}(t) + \mathbf{B_{dq}} \cdot \mathbf{u_{dq}}(t) \\ \mathbf{y_{dq}}(t) = \mathbf{C_{dq}} \cdot \mathbf{q_{dq}}(t) + \mathbf{D_{dq}} \cdot \mathbf{u_{dq}}(t) \end{cases} \quad (23)$$

In this model, $\mathbf{q_{dq}}(t)$, $\mathbf{y_{dq}}(t)$, and $\mathbf{u_{dq}}(t)$ represent the state, output, and input vectors in dq coordinates, respectively. Specifically, $\mathbf{q_{dq}}(t) = [q_{1d}(t), q_{1q}(t), q_{2d}(t), q_{2q}(t)]^{\mathrm{T}}$, $\mathbf{y_{dq}}(t) = \mathbf{q_{dq}}(t)$, and $\mathbf{u_{dq}}(t) = [u_{1d}(t), u_{1q}(t)]^{\mathrm{T}}$. These vectors can also be defined as $\{\mathbf{q_{dq}}(t), \mathbf{y_{dq}}(t)\} \in \{\mathbb{R}^4\}$ and $\mathbf{u_{dq}}(t) \in \{\mathbb{R}^2\}$. The matrices $\mathbf{A_{dq}}$, $\mathbf{B_{dq}}$ are as described as follows

$$\mathbf{A_{dq}} = \begin{bmatrix} 0 & \omega & 1 & 0 \\ -\omega & 0 & 0 & 1 \\ -\dfrac{k_{eq_1}}{m_1} & 0 & -\dfrac{b_{eq_1}}{m_1} & \omega \\ 0 & -\dfrac{k_{eq_1}}{m_1} & -\omega & -\dfrac{b_{eq_1}}{m_1} \end{bmatrix}$$

$$\mathbf{B_{dq}} = \begin{bmatrix} 0 & 0 \\ 0 & 0 \\ \dfrac{1}{m_1} & 0 \\ 0 & \dfrac{1}{m_1} \end{bmatrix} \quad (24)$$

and the matrices $\mathbf{C_{dq}}$ and $\mathbf{D_{dq}}$ are identity and zero, respectively. Here, ω represents the angular frequency corresponding to the excitation force. Symbolically, the matrices can be defined as $\{\mathbf{A_{dq}}, \mathbf{C_{dq}}\} \in \mathscr{M}_{4\times4}$ and $\{\mathbf{B_{dq}}, \mathbf{D_{dq}}\} \in \mathscr{M}_{4\times1}$.

Extending this model, a linear electrical analogy can be derived to represent the mechanical system. The electrical model is shown in Fig. 3 and is developed for both the d and q channels. Each electrical network is configured using equivalent Thevenin circuits consisting of energy-storing elements (m_1 as inductor and $1/k_{eq1}$ as capacitor) and voltage sources controlled by charges ($q_{1j}(t)$ and $q_{2j}(t)$, where $j \in \{d, q\}$).
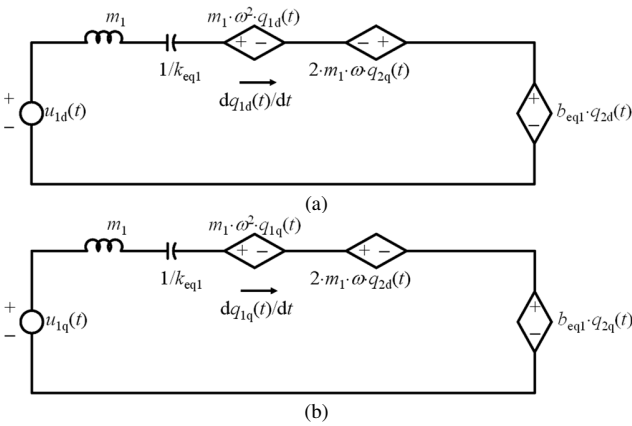

(a)

(b)

Fig. 3. Electrical analogy of the proposed 1-DoF mechanical system in dq coordinates. The two channels d and q are shown. (a) Channel d. (b) Channel q.

B. Analysis of a Mechanical Vibrational Dynamical System of Two-Degree-of-Freedom

This section presents the analysis of a 2-DoF vibrational mechanical system, as shown in Fig. 2(b). Following the methodology used for the 1-DoF system, the energy equations for this 2-DoF system are derived and given by

$$\begin{cases} KE(t) = \dfrac{1}{2} \cdot m_1 \cdot \dot{x}_1(t)^2 + \dfrac{1}{2} \cdot m_2 \cdot \dot{x}_2(t)^2 \\ PE(t) = \dfrac{1}{2} \cdot k_{eq_1} \cdot x_1(t)^2 - k_2 \cdot x_1(t) \cdot x_2(t) + \\ \qquad + \dfrac{1}{2} \cdot k_{eq_2} \cdot x_2(t)^2 \\ DE(t) = \dfrac{1}{2} \cdot b_{eq_1} \cdot \dot{x}_1(t)^2 - b_2 \cdot \dot{x}_1(t) \cdot \dot{x}_2(t) + \\ \qquad + \dfrac{1}{2} \cdot b_{eq_2} \cdot \dot{x}_2(t)^2 \end{cases} \quad (25)$$

Also, $b_{eq1} = b_1 + b_2$, $b_{eq2} = b_2 + b_3$, $k_{eq1} = k_1 + k_2$, and $k_{eq2} = k_2 + k_3$.

Now, using these energy expressions and applying (17) with $p_1(t) = x_1(t)$ and $p_2(t) = x_2(t)$, after some algebraic manipulations, the model of the 2-DoF system in mechanical coordinates in state-space representation is obtained, which is defined in (18). To maintain generality, it is worth noting that and, the matrices $\mathbf{C}$ and $\mathbf{D}$ are the identity and zero matrices, the vector and matrix model of a vibrating system in mechanical coordinates in state-space representation follows the same respectively. Mathematically, $\{\mathbf{A}, \mathbf{C}\} \in \mathscr{M}_{4\times4}$ and $\{\mathbf{B}, \mathbf{D}\} \in \mathscr{M}_{4\times1}$ where $\mathbf{A}$, $\mathbf{B}$, $\mathbf{C}$, and $\mathbf{D}$ are the state matrix, input matrix, output matrix, and direct transmission matrix, respectively.

In this case, the model vectors in (18) are as follows: the state vector $\mathbf{q}(t) = [q_1(t), q_2(t), q_3(t), q_4(t)]^{\mathrm{T}}$, the output vector $\mathbf{y}(t) = \mathbf{q}(t)$, and the scalar input $u(t) = f_1(t)$. Moreover, $q_1(t) = x_1(t)$, $q_2(t) = dx_1(t)/dt$, $q_3(t) = x_2(t)$, and $q_4(t) = dx_2(t)/dt$. Symbolically, $\{\mathbf{q}(t), \mathbf{y}(t)\} \in \{\mathbb{R}^4\}$.

The model matrices in (18) are defined as follows

$$\mathbf{A} = \begin{bmatrix} 0 & 1 & 0 & 0 \\ -\dfrac{k_{eq_1}}{m_1} & -\dfrac{b_{eq_1}}{m_1} & \dfrac{k_2}{m_1} & \dfrac{b_2}{m_1} \\ 0 & 0 & 0 & 1 \\ \dfrac{k_2}{m_2} & \dfrac{b_2}{m_2} & -\dfrac{k_{eq_2}}{m_2} & -\dfrac{b_{eq_2}}{m_2} \end{bmatrix}$$

$$\mathbf{B} = \begin{bmatrix} 0 \\ 0 \\ 0 \\ \dfrac{1}{m_2} \end{bmatrix} \quad (26)$$

The model (18) is then converted into αβ coordinates using the procedure developed previously in the 1-DoF system analysis. The equivalences defined in (27) are used to perform this transformation. The resulting 2-DoF vibrational mechanical system in αβ coordinates in state space format is defined in (21). As with the development of the model (18), it

$$\begin{cases} q_{1\alpha}(t) = q_1(t) \\ q_{1\beta}(t) = q_1\left(t - \dfrac{\pi}{2}\right) \\ q_{2\alpha}(t) = q_2(t) \\ q_{2\beta}(t) = q_2\left(t - \dfrac{\pi}{2}\right) \\ q_{3\alpha}(t) = q_3(t) \\ q_{3\beta}(t) = q_3\left(t - \dfrac{\pi}{2}\right) \\ q_{4\alpha}(t) = q_4(t) \\ q_{4\beta}(t) = q_4\left(t - \dfrac{\pi}{2}\right) \\ u_\alpha(t) = u(t) \\ u_\beta(t) = u\left(t - \dfrac{\pi}{2}\right) \end{cases} \quad (27)$$

can be observed that the model of the system in αβ coordinates in state-space representation follows the same structure as that defined in (21) for a generalized n-DoF system.

The vectors involved in (21) are defined as follows: $\mathbf{q}_{\alpha\beta}(t)$ = $[q_{1\alpha}(t), q_{1\beta}(t), q_{2\alpha}(t), q_{2\beta}(t), q_{3\alpha}(t), q_{3\beta}(t), q_{4\alpha}(t), q_{4\beta}(t)]^T$, $\mathbf{y}_{\alpha\beta}(t)$ = $\mathbf{q}_{\alpha\beta}(t)$, and $\mathbf{u}_{\alpha\beta}(t) = [u_{1\alpha}(t), u_{1\beta}(t)]^T$, where $\mathbf{q}_{\alpha\beta}(t)$, $\mathbf{y}_{\alpha\beta}(t)$, and $\mathbf{u}_{\alpha\beta}(t)$ are the state, output, and input vectors, respectively. Symbolically, $\{\mathbf{q}_{\alpha\beta}(t), \mathbf{y}_{\alpha\beta}(t)\} \in \{\mathbb{R}^8\}$ and $\mathbf{u}_{\alpha\beta}(t) \in \{\mathbb{R}^2\}$. The model matrices in (21) are $\mathbf{A}_{\alpha\beta}$, $\mathbf{B}_{\alpha\beta}$, which correspond to the state and input matrices given by

$$\mathbf{A}_{\alpha\beta} = \left[\begin{array}{cccc|cccc} 0 & 0 & 1 & 0 & 0 & 0 & 0 & 0 \\ 0 & 0 & 0 & 1 & 0 & 0 & 0 & 0 \\ -\dfrac{k_{eq_1}}{m_1} & 0 & -\dfrac{b_{eq_1}}{m_1} & 0 & \dfrac{k_2}{m_1} & \dfrac{k_2}{m_1} & \dfrac{b_2}{m_1} & 0 \\ 0 & -\dfrac{k_{eq_1}}{m_1} & 0 & -\dfrac{b_{eq_1}}{m_1} & 0 & 0 & 0 & \dfrac{b_2}{m_1} \\ 0 & 0 & 0 & 0 & 0 & 0 & 1 & 0 \\ 0 & 0 & 0 & 0 & 0 & 0 & 0 & 1 \\ \dfrac{k_2}{m_2} & 0 & \dfrac{b_2}{m_2} & 0 & -\dfrac{k_{eq_2}}{m_2} & 0 & -\dfrac{b_{eq_2}}{m_2} & 0 \\ 0 & \dfrac{k_2}{m_2} & 0 & \dfrac{b_2}{m_2} & 0 & -\dfrac{k_{eq_2}}{m_2} & 0 & -\dfrac{b_{eq_2}}{m_2} \end{array}\right] \quad (28a)$$

$$\mathbf{B}_{\alpha\beta} = \begin{bmatrix} 0 & 0 \\ 0 & 0 \\ 0 & 0 \\ 0 & 0 \\ 0 & 0 \\ 0 & 0 \\ \dfrac{1}{m_2} & 0 \\ 0 & \dfrac{1}{m_2} \end{bmatrix} \quad (28b)$$

and (28b), respectively. In addition, $\mathbf{C}_{\alpha\beta}$ and $\mathbf{D}_{\alpha\beta}$ are the output and direct transmission matrices representing the identity and zero matrices, respectively. Symbolically, $\{\mathbf{A}_{\alpha\beta}, \mathbf{C}_{\alpha\beta}\} \in \mathcal{M}_{8\times8}$ and $\{\mathbf{B}_{\alpha\beta}, \mathbf{D}_{\alpha\beta}\} \in \mathcal{M}_{8\times2}$.

In the final step, this model in αβ coordinates is transformed into dq coordinates. Similar to the 1-DoF system analysis, the $\mathbf{K_p}$ matrix is applied to (21) to obtain the model of the 2-DoF vibrational mechanical system in dq coordinates in the state-space representation defined in (23). It is important to note that the vector and matrix model for an n-DoF mechanical system follows the same structure as shown in (23).

The vectors of the model (23) in dq coordinates are defined as follows: $\mathbf{q}_{dq}(t) = [q_{1d}(t), q_{1q}(t), q_{2d}(t), q_{2q}(t), q_{3d}(t), q_{4d}(t), q_{4q}(t)]^T$, $\mathbf{y}_{dq}(t) = \mathbf{q}_{dq}(t)$, and $\mathbf{u}_{dq}(t) = [u_{1d}(t), u_{1q}(t)]^T$, and they refer to the state, output, and input vectors, respectively. Mathematically, $\{\mathbf{q}_{dq}(t), \mathbf{y}_{dq}(t)\} \in \{\mathbb{R}^8\}$ and $\mathbf{u}_{dq}(t) \in \{\mathbb{R}^2\}$.

As with the 1-DoF system, the electrical analog model for the 2-DoF system is obtained as shown in Fig. 4. These circuits, similar to the 1-DoF system, are based on Thévenin voltage models. Specifically, Fig. 4(a) and (b) show the electrical diagrams of the d and q channels, respectively. Note that the 2-DoF system has two state variables per channel, twice as many as in the 1-DoF case.

Analysis of a Mechanical Vibrational Dynamical System of Three-Degree-of-Freedom

This section presents an analysis of a 3-DoF mechanical vibration system, as shown in Fig. 2(c). The energy equations governing this 3-DoF system, expressed as follows

$$\begin{cases} KE(t) = \dfrac{1}{2} \cdot m_1 \cdot \dot{x}_1(t)^2 + \dfrac{1}{2} \cdot m_2 \cdot \dot{x}_2(t)^2 + \\ \qquad\qquad + \dfrac{1}{2} \cdot m_3 \cdot \dot{x}_3(t)^2 \\ PE(t) = \dfrac{1}{2} \cdot k_{eq_1} \cdot x_1(t)^2 + \dfrac{1}{2} \cdot k_{eq_2} \cdot x_2(t)^2 + \\ \qquad + \dfrac{1}{2} \cdot k_{eq_3} \cdot x_3(t)^2 - k_2 \cdot x_1(t) \cdot x_2(t) - \\ \qquad\qquad - k_3 \cdot x_2(t) \cdot x_3(t) \\ DE(t) = \dfrac{1}{2} \cdot b_{eq_1} \cdot \dot{x}_1(t)^2 + \dfrac{1}{2} \cdot b_{eq_2} \cdot \dot{x}_2(t)^2 + \\ \qquad + \dfrac{1}{2} \cdot b_{eq_3} \cdot \dot{x}_3(t)^2 - b_2 \cdot \dot{x}_1(t) \cdot \dot{x}_2(t) - \\ \qquad\qquad - b_3 \cdot \dot{x}_2(t) \cdot \dot{x}_3(t) \end{cases} \quad (29)$$

are derived similarly to the 1- and 2-DoF systems.

In particular, the energy equations include parameters such as $b_{eq1} = b_1 + b_2$, $b_{eq2} = b_2 + b_3$, $b_{eq3} = b_3 + b_4$, $k_{eq1} = k_1 + k_2$, $k_{eq2} = k_2 + k_3$, and $k_{eq3} = k_3 + k_4$.

By applying (17) to these energy expressions, a state-space dynamical model is formulated as defined in (18). Within this model, the state vector $\mathbf{q}(t) = [q_j(t)]^\mathrm{T}$, where $j \in \{1, 2, 3, 4, 5, 6\}$, and the output vector $\mathbf{y}(t) = \mathbf{q}(t)$. The individual components

of the state vector, such as $q_1(t) = x_1(t)$, $q_2(t) = dx_1(t)/dt$, $q_3(t) = x_2(t)$, $q_4(t) = dx_2(t)/dt$, $q_5(t) = x_3(t)$, and $q_6(t) = dx_3(t)/dt$, are detailed. In addition, the scalar input is denoted by $u(t) = f_1(t)$. Symbolically, this system is characterized as $\{\mathbf{q}(t), \mathbf{y}(t)\} \in \{\mathbb{R}^6\}$. The state matrix ($\mathbf{A}$) and the input matrix ($\mathbf{B}$) are defined as follows

$$\mathbf{A} = \begin{bmatrix} 0 & 1 & 0 & 0 \\ -\dfrac{k_{eq_1}}{m_1} & -\dfrac{b_{eq_1}}{m_1} & \dfrac{k_2}{m_1} & \dfrac{b_2}{m_1} \\ 0 & 0 & 0 & 1 \\ \dfrac{k_2}{m_2} & \dfrac{b_2}{m_1} & -\dfrac{k_{eq_2}}{m_2} & -\dfrac{b_{eq_2}}{m_2} \\ 0 & 0 & 0 & 0 \\ 0 & 0 & \dfrac{k_{eq_3}}{m_3} & \dfrac{b_3}{m_3} \end{bmatrix}$$

$$\begin{matrix} 0 & 0 \\ 0 & 0 \\ 0 & 0 \\ \dfrac{k_{eq_3}}{m_2} & \dfrac{b_3}{m_2} \\ 0 & 1 \\ -\dfrac{k_{eq_3}}{m_3} & -\dfrac{b_{eq_3}}{m_3} \end{matrix} \qquad (30)$$

$$\mathbf{B} = \begin{bmatrix} 0 \\ 0 \\ 0 \\ 0 \\ 0 \\ \dfrac{1}{m_3} \end{bmatrix}$$

while the output matrix ($\mathbf{C}$) and the direct transmission matrix ($\mathbf{D}$) are both identity and zero matrices, respectively. This representation can be expressed as $\{\mathbf{A}, \mathbf{C}\} \in \mathcal{M}_{6\times6}$ and $\{\mathbf{B}, \mathbf{D}\} \in \mathcal{M}_{6\times1}$.

To further analyze the system, a transformation into $\alpha\beta$ coordinates is performed, following a similar approach to the 1- and 2-DoF systems. The transformation process, defined in (21), includes notations such as $q_{i\alpha}(t) = q_i(t)$ and $q_{i\beta}(t) = q_i(t - \pi/2)$, as well as $u_\alpha(t) = u(t)$ and $u_\beta(t) = u(t - \pi/2)$. This transformation yields new state ($\mathbf{q}_{\alpha\beta}(t)$), input ($\mathbf{u}_{\alpha\beta}(t)$), and output ($\mathbf{y}_{\alpha\beta}(t)$) vectors, represented as $\mathbf{q}_{\alpha\beta}(t) = [q_{i\alpha}(t), q_{i\beta}(t)]^\mathrm{T}$ for $i \in \{1, 2, 3, 4, 5, 6\}$, $\mathbf{y}_{\alpha\beta}(t) = \mathbf{q}_{\alpha\beta}(t)$, and $\mathbf{u}_{\alpha\beta}(t) = [u_\alpha(t), u_\beta(t)]^\mathrm{T}$. In this context, $\{\mathbf{q}_{\alpha\beta}(t), \mathbf{y}_{\alpha\beta}(t)\} \in \{\mathbb{R}^{12}\}$ and $\mathbf{u}_{\alpha\beta}(t) \in \{\mathbb{R}^2\}$. The model matrices from (21), denoted $\mathbf{A}_{\alpha\beta}$ and $B_{\alpha\beta}$, reflect the state and input matrices, respectively which are given by

$$\mathbf{A}_{\alpha\beta} = \begin{bmatrix} \mathbf{A}_{\alpha\beta_{11}} & \mathbf{A}_{\alpha\beta_{12}} \\ \mathbf{A}_{\alpha\beta_{21}} & \mathbf{A}_{\alpha\beta_{22}} \end{bmatrix}$$

$$\mathbf{B}_{\alpha\beta} = \begin{bmatrix} \mathbf{B}_{\alpha\beta_{11}} \\ \mathbf{B}_{\alpha\beta_{21}} \end{bmatrix} \qquad (31)$$

Moreover, the output matrix $\mathbf{C}_{\alpha\beta}$ and the direct transmission matrix $\mathbf{D}_{\alpha\beta}$ retain their identity and zero-matrix properties. The
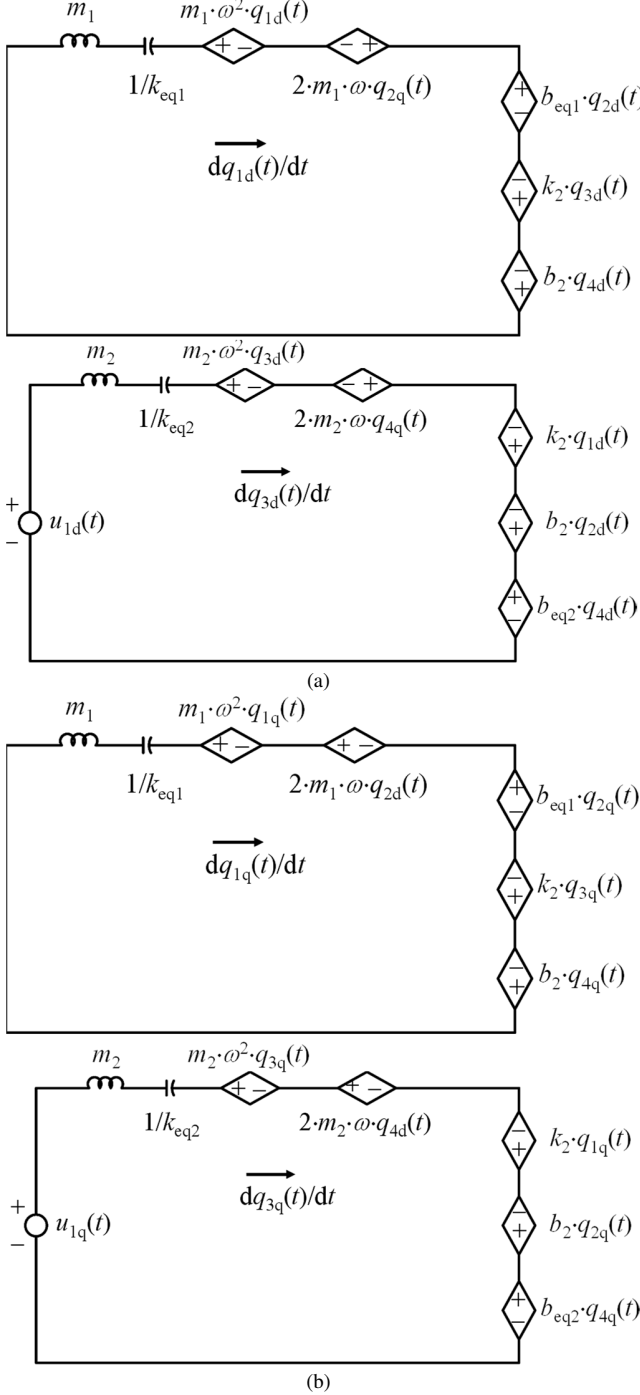
Fig. 4. Electrical analogy of the proposed 2-DoF mechanical system in dq coordinates. The two channels d and q are shown. (a) Channel d. (b) Channel q.

submatrices of $\mathbf{A}_{\alpha\beta ij}$ and $\mathbf{B}_{\alpha\beta ij}$, , where $\{i,j\} \in \{1,2\}$ are defined as follows

$$\mathbf{A}_{\alpha\beta 11} = \begin{bmatrix} 0 & 0 & 1 & 0 & 0 & 0 \\ 0 & 0 & 0 & 1 & 0 & 0 \\ -\dfrac{k_{eq_1}}{m_1} & 0 & -\dfrac{b_{eq_1}}{m_1} & 0 & \dfrac{k_2}{m_1} & 0 \\ 0 & -\dfrac{k_{eq_1}}{m_1} & 0 & -\dfrac{b_{eq_1}}{m_1} & 0 & \dfrac{k_2}{m_1} \\ 0 & 0 & 0 & 0 & 0 & 0 \\ 0 & 0 & 0 & 0 & 0 & 0 \end{bmatrix}$$

$$\mathbf{A}_{\alpha\beta 12} = \begin{bmatrix} 0 & 0 & 0 & 0 & 0 & 0 \\ 0 & 0 & 0 & 0 & 0 & 0 \\ \dfrac{b_2}{m_1} & 0 & 0 & 0 & 0 & 0 \\ 0 & \dfrac{b_2}{m_1} & 0 & 0 & 0 & 0 \\ 0 & 0 & 0 & 0 & 0 & 0 \\ 1 & 0 & 0 & 0 & 0 & 0 \end{bmatrix}$$

$$\mathbf{A}_{\alpha\beta 21} = \begin{bmatrix} \dfrac{k_2}{m_2} & 0 & \dfrac{b_2}{m_2} & 0 & -\dfrac{k_{eq_2}}{m_2} & 0 \\ 0 & \dfrac{k_2}{m_2} & 0 & \dfrac{b_2}{m_2} & 0 & -\dfrac{k_{eq_2}}{m_2} \\ 0 & 0 & 0 & 0 & 0 & 0 \\ 0 & 0 & 0 & 0 & 0 & 0 \\ 0 & 0 & 0 & 0 & \dfrac{k_3}{m_3} & 0 \\ 0 & 0 & 0 & 0 & 0 & \dfrac{k_3}{m_3} \end{bmatrix}$$

$$\mathbf{A}_{\alpha\beta 22} =$$
$$\begin{bmatrix} -\dfrac{b_{eq_2}}{m_2} & 0 & \dfrac{k_3}{m_2} & 0 & \dfrac{b_3}{m_2} & 0 \\ 0 & -\dfrac{b_{eq_2}}{m_2} & 0 & \dfrac{k_3}{m_2} & 0 & \dfrac{b_3}{m_2} \\ 0 & 0 & 0 & 0 & 1 & 0 \\ 0 & 0 & 0 & 0 & 0 & 1 \\ \dfrac{b_3}{m_3} & 0 & -\dfrac{k_{eq_3}}{m_3} & 0 & -\dfrac{b_{eq_3}}{m_3} & 0 \\ 0 & \dfrac{b_3}{m_3} & 0 & -\dfrac{k_{eq_3}}{m_3} & 0 & -\dfrac{b_{eq_3}}{m_3} \end{bmatrix}$$

(32)

$$\mathbf{B}_{\alpha\beta 11} = \mathbf{0}$$

$$\mathbf{B}_{\alpha\beta 21} = \begin{bmatrix} 0 & 0 \\ 0 & 0 \\ 0 & 0 \\ 0 & 0 \\ \dfrac{1}{m_3} & 0 \\ 0 & \dfrac{1}{m_3} \end{bmatrix}$$

(33)

Symbolically, $\{\mathbf{A}_{\alpha\beta}, \mathbf{C}_{\alpha\beta}\} \in \mathcal{M}_{12\times 12}$ and $\{\mathbf{B}_{\alpha\beta}, \mathbf{D}_{\alpha\beta}\} \in \mathcal{M}_{12\times 2}$.

A final transformation to dq coordinates is performed,

similar to the approaches used for the 1- and 2-DoF systems. By applying the $\mathbf{K_p}$ matrix to (21), the state-space representation of the 3-DoF vibrational mechanical system in dq coordinates is established and outlined in (23). Within this representation, the state vector ($\mathbf{q_{dq}}(t)$), the output vector ($\mathbf{y_{dq}}(t)$), and the input vector ($\mathbf{u_{dq}}(t)$) are defined as $\mathbf{q_{dq}}(t) = [q_{id}(t), q_{iq}(t)]^{\mathrm{T}}$ for $i \in \{1, 2, 3, 4, 5, 6\}$, $\mathbf{y_{dq}}(t) = \mathbf{q_{dq}}(t)$, and $\mathbf{u_{dq}}(t) = [u_d(t), u_q(t)]^{\mathrm{T}}$. Mathematically, this system can be described as $\{\mathbf{q_{dq}}(t), \mathbf{y_{dq}}(t)\} \in \{\mathbb{R}^{12}\}$, with $\mathbf{u_{dq}}(t) \in \{\mathbb{R}^2\}$.

Once the model described in (21) has been calculated and using the same procedure as for the 1- and 2-DoF cases, the dynamical system in dq-domain state-space representation for the 3-DoF system is derived and defined in (23). The state ($\mathbf{q_{dq}}(t)$), output ($\mathbf{y_{dq}}(t)$), and input ($\mathbf{u_{dq}}(t)$) vectors are defined as follows; $\mathbf{q_{dq}}(t) = [q_{id}(t), q_{iq}(t)]^{\mathrm{T}}$ for $i \in \{1, 2, 3, 4, 5, 6\}$, $\mathbf{y_{dq}}(t) = \mathbf{q_{dq}}(t)$, and $\mathbf{u_{dq}}(t) = [u_d(t), u_q(t)]^{\mathrm{T}}$. Mathematically, $\{\mathbf{q_{dq}}(t), \mathbf{y_{dq}}(t)\} \in \{\mathbb{R}^{12}\}$ and $\mathbf{u_{dq}}(t) \in \{\mathbb{R}^2\}$. The definitions of the state ($\mathbf{A_{dq}}$) and input ($\mathbf{B_{dq}}$) matrices are defined by

$$\mathbf{A_{dq}} = \begin{bmatrix} \mathbf{A_{dq11}} & \mathbf{A_{dq12}} \\ \mathbf{A_{dq21}} & \mathbf{A_{dq22}} \end{bmatrix}$$
$$\mathbf{B_{dq}} = \begin{bmatrix} \mathbf{B_{dq11}} \\ \mathbf{B_{dq21}} \end{bmatrix}$$

(34)

where the output ($\mathbf{C_{dq}}$) and direct transmission ($\mathbf{D_{dq}}$) matrices are the identity and zero matrices, respectively. The submatrices of $\mathbf{A_{dq}}_{ij}$ and $\mathbf{B_{dq}}_{ij}$, , where $\{i, j\} \in \{1, 2\}$ are given by (35) and (36).

Additionally, an electrical analog model for the 3-DoF system is developed based on Thévenin voltage circuits, considering (23), as shown in Fig. 5. The d and q channels are shown separately in Fig. 5(a) and (b).

A notable observation from the analysis of the 1-, 2-, and 3-DoF models is that they all maintain their linearity regardless of the transformation applied. This is because the original mechanical systems are linear, and the transformations are inherently linear processes, leading to linear systems [35], [36]. In addition, the models in dq coordinates have coupling between them, which can be eliminated by nodal transformations, resulting in uncoupled equations based on the respective eigenvalues [37]. Finally, the analog electrical circuit models can be considered for implementation in simulation programs, facilitating the analysis of their behavior.

IV. ANALYSIS OF ENERGY EQUATIONS: MECHANICAL ENERGY CURVES AND dq ENERGY SURFACES IN 1-, 2-, AND 3-DoF SYSTEMS

The analysis of energy equations in mechanical and dq coordinates for vibrating mechanical systems with 1-, 2-, and 3-DoF holds great value. This study reveals complex system dynamics, quantifies energy losses, provides comparative insights, aids in control and optimization, identifies resonances, serves as an educational tool, and expands its relevance to interdisciplinary fields. This comprehensive analysis enhances the understanding of mechanical systems and contributes to the advancement of engineering [38], [39].

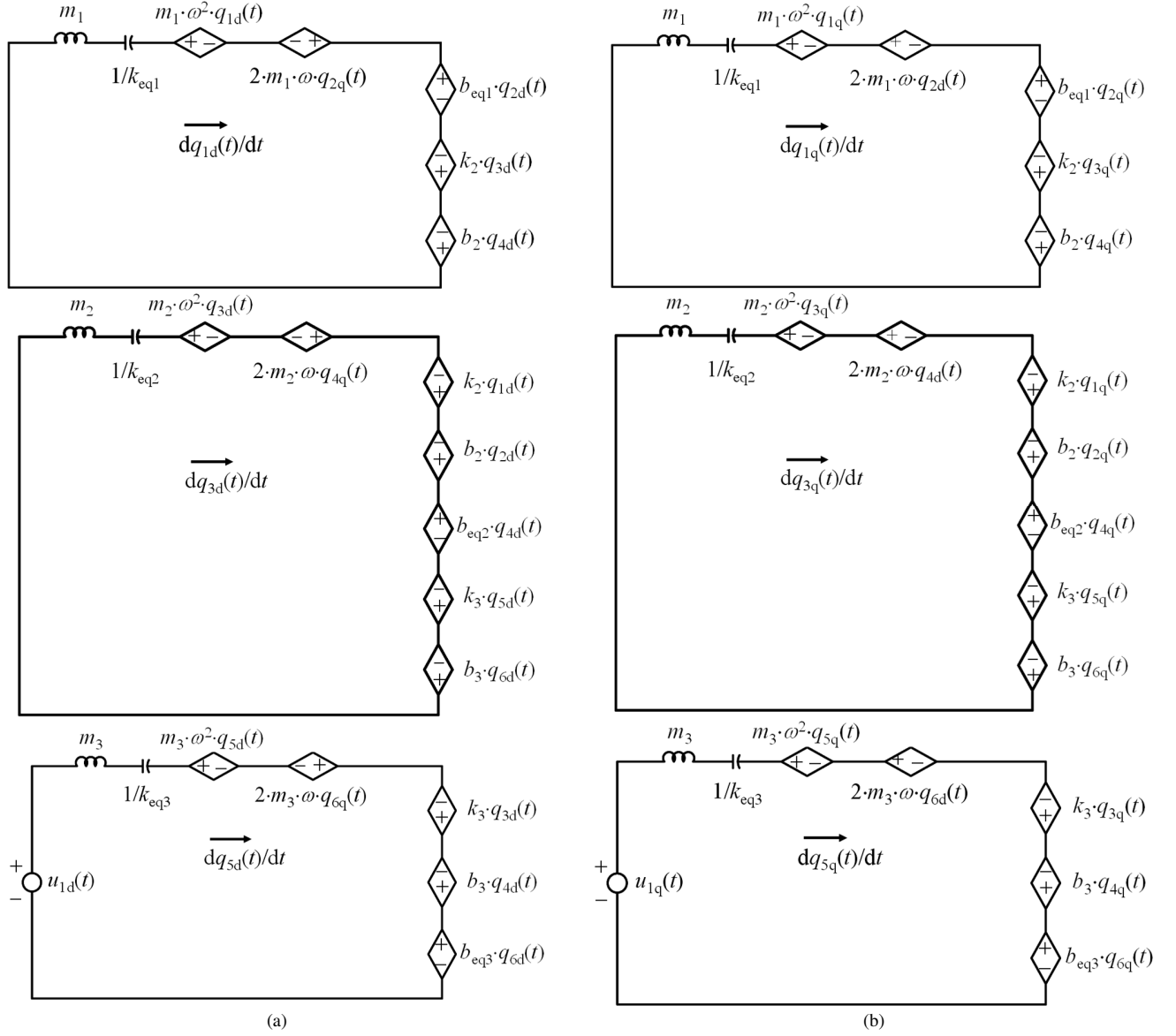In this study, the expressions of the energies involved in

Fig. 5. Electrical analogy of the proposed 3-DoF mechanical system in dq coordinates. The two channels d and q are shown. (a) Channel d. (b) Channel q.

mechanical coordinates have already been obtained for the 1-DoF system (16), for the 2-DoF system (25), and for the 3-DoF system (29), so the dq-coordinate versions of these expressions are computed below. Derivation of the expressions for the kinetic, potential, and dissipation energies involved in the 1-DoF system.

To simplify the analysis, the energy equations in mechanical coordinates, related to the 1-DoF system (16), are again presented in (37).

First, the transformation of $KE(t)$ is considered. According to the development presented throughout the study in converting dynamical systems in mechanical coordinates to alphabetic coordinates, the expression of $KE(t)$ in $\alpha\beta$ coordinates can be considered in (38).

The application of $\mathbf{K_p}$ to (38) gives the $KE_{dq}(t)$ expression in (39). Applying the same procedure to the expressions of

$PE(t)$ and $DE(t)$, these expressions can be expressed in dq coordinates in (40).

A. *Derivation of the expressions for the kinetic, potential, and dissipation energies involved in the 2-DoF system*

Applying the same procedure developed in the case of 1-DoF, the expressions of $KE(t)$, $PE(t)$, and $DE(t)$ in dq coordinates related to the case of the 2-DoF system are obtained and defined in (41).

B. *Derivation of the expressions for the kinetic, potential, and dissipation energies involved in the 3-DoF system*

Applying the same procedure developed in the case of 1-DoF, the expressions of $KE(t)$, $PE(t)$, and $DE(t)$ in dq coordinates related to the case of the 3-DoF system are obtained in (42).

$$\mathbf{A_{dq11}} = \begin{bmatrix} 0 & \omega & 1 & 0 & 0 & 0 \\ -\omega & 0 & 0 & 1 & 0 & 0 \\ -\dfrac{k_{eq_1}}{m_1} & 0 & -\dfrac{b_{eq_1}}{m_1} & \omega & \dfrac{k_2}{m_1} & 0 \\ 0 & -\dfrac{k_{eq_1}}{m_1} & -\omega & -\dfrac{b_{eq_1}}{m_1} & 0 & \dfrac{k_2}{m_1} \\ 0 & 0 & 0 & 0 & 0 & \omega \\ 0 & 0 & 0 & 0 & -\omega & 0 \end{bmatrix}$$

$$\mathbf{A_{dq12}} = \begin{bmatrix} 0 & 0 & 0 & 0 & 0 & 0 \\ 0 & 0 & 0 & 0 & 0 & 0 \\ \dfrac{b_2}{m_1} & 0 & 0 & 0 & 0 & 0 \\ 0 & \dfrac{b_2}{m_1} & 0 & 0 & 0 & 0 \\ 1 & 0 & 0 & 0 & 0 & 0 \\ 0 & 1 & 0 & 0 & 0 & 0 \end{bmatrix}$$

$$\mathbf{A_{dq21}} = \begin{bmatrix} \dfrac{k_2}{m_2} & 0 & \dfrac{b_2}{m_2} & 0 & -\dfrac{k_{eq_2}}{m_2} & 0 \\ 0 & \dfrac{k_2}{m_2} & 0 & \dfrac{b_2}{m_2} & 0 & -\dfrac{k_{eq_2}}{m_2} \\ 0 & 0 & 0 & 0 & 0 & 0 \\ 0 & 0 & 0 & 0 & 0 & 0 \\ 0 & 0 & 0 & 0 & \dfrac{k_3}{m_3} & 0 \\ 0 & 0 & 0 & 0 & 0 & \dfrac{k_3}{m_3} \end{bmatrix}$$

$$\mathbf{A_{dq22}} =$$
$$= \begin{bmatrix} -\dfrac{b_{eq_2}}{m_2} & \omega & \dfrac{k_3}{m_2} & 0 & \dfrac{b_3}{m_2} & 0 \\ -\omega & -\dfrac{b_{eq_2}}{m_2} & 0 & \dfrac{k_3}{m_2} & 0 & \dfrac{b_3}{m_2} \\ 0 & 0 & 0 & \omega & 1 & 0 \\ 0 & 0 & -\omega & 0 & 0 & 1 \\ \dfrac{b_3}{m_3} & 0 & -\dfrac{k_{eq_3}}{m_3} & 0 & -\dfrac{b_{eq_3}}{m_3} & \omega \\ 0 & \dfrac{b_3}{m_3} & 0 & -\dfrac{k_{eq_3}}{m_3} & -\omega & -\dfrac{b_{eq_3}}{m_3} \end{bmatrix}$$
$$(35)$$

$$\mathbf{B_{dq11}} = \mathbf{B_{\alpha\beta11}}$$
$$\mathbf{B_{dq21}} = \mathbf{B_{\alpha\beta21}}$$
$$(36)$$

$$\begin{cases} KE(t) = \dfrac{1}{2} \cdot m_1 \cdot \dot{x}_1(t)^2 \\ PE(t) = \dfrac{1}{2} \cdot k_{eq_1} \cdot x_1(t)^2 \\ DE(t) = \dfrac{1}{2} \cdot b_{eq_1} \cdot \dot{x}_1(t)^2 \end{cases} \quad (37)$$

$$KE_{\alpha\beta}(t) = \dfrac{1}{2} \cdot m_1 \cdot [\dot{x}_{1\alpha}(t) \quad \dot{x}_{1\beta}(t)] \cdot \begin{bmatrix} \dot{x}_{1\alpha}(t) \\ \dot{x}_{1\beta}(t) \end{bmatrix}^{\mathrm{T}} \quad (38)$$

V. Solution of the System in Mechanical and dq Coordinates

To gain a thorough insight into the dynamics of the state variables of the systems studied so far, both in the domain in mechanical coordinates and in the domain in dq coordinates, it

$$\begin{cases} KE_{dq}(t) = \dfrac{1}{2} \cdot m_1 \cdot \left(\mathbf{K_p} \cdot \begin{bmatrix} \dot{x}_{1d}(t) \\ \dot{x}_{1q}(t) \end{bmatrix} \right)^{\mathrm{T}} \cdot \mathbf{K_p} \cdot \begin{bmatrix} \dot{x}_{1d}(t) \\ \dot{x}_{1q}(t) \end{bmatrix} \\ KE_{dq}(t) = \dfrac{1}{2} \cdot m_1 \cdot [\dot{x}_{1d}(t) \quad \dot{x}_{1q}(t)] \cdot \mathbf{K_p}^{\mathrm{T}} \cdot \mathbf{K_p} \cdot \begin{bmatrix} \dot{x}_{1d}(t) \\ \dot{x}_{1q}(t) \end{bmatrix} \\ \qquad KE_{dq}(t) = \dfrac{1}{2} \cdot m_1 \cdot \left(\dot{x}_{1d}(t)^2 + \dot{x}_{1q}(t)^2 \right) \end{cases}$$
$$(39)$$

$$\begin{cases} PE_{dq}(t) = \dfrac{1}{2} \cdot k_{eq_1} \cdot \left(x_{1d}(t)^2 + x_{1q}(t)^2 \right) \\ DE_{dq}(t) = \dfrac{1}{2} \cdot b_{eq_1} \cdot \left(\dot{x}_{1d}(t)^2 + \dot{x}_{1q}(t)^2 \right) \end{cases} \quad (40)$$

$$\begin{cases} KE_{dq}(t) = \dfrac{1}{2} \cdot m_1 \cdot \left(\dot{x}_{1d}(t)^2 + \dot{x}_{1q}(t)^2 \right) + \\ \quad + \dfrac{1}{2} \cdot m_2 \cdot \left(\dot{x}_{2d}(t)^2 + \dot{x}_{2q}(t)^2 \right) \\ PE_{dq}(t) = \dfrac{1}{2} \cdot k_{eq_1} \cdot \left(x_{1d}(t)^2 + x_{1q}(t)^2 \right) - \\ \quad -k_2 \cdot \left(x_{1d}(t) \cdot x_{2d}(t) + x_{1q}(t) \cdot x_{2q}(t) \right) + \\ \quad + \dfrac{1}{2} \cdot k_{eq_2} \cdot \left(x_{2d}(t)^2 + x_{2q}(t)^2 \right) \\ DE_{dq}(t) = \dfrac{1}{2} \cdot b_{eq_1} \cdot \left(\dot{x}_{1d}(t)^2 + \dot{x}_{1q}(t)^2 \right) - \\ \quad -b_2 \cdot \left(\dot{x}_{1d}(t) \cdot \dot{x}_{2d}(t) + \dot{x}_{1q}(t) \cdot \dot{x}_{2q}(t) \right) + \\ \quad \dfrac{1}{2} \cdot b_{eq_2} \cdot \left(\dot{x}_{2d}(t)^2 + \dot{x}_{2q}(t)^2 \right) \end{cases} \quad (41)$$

$$\begin{cases} KE_{dq}(t) = \dfrac{1}{2} \cdot m_1 \cdot \left(\dot{x}_{1d}(t)^2 + \dot{x}_{1q}(t)^2 \right) + \\ \quad + \dfrac{1}{2} \cdot m_2 \cdot \left(\dot{x}_{2d}(t)^2 + \dot{x}_{2q}(t)^2 \right) + \\ \quad + \dfrac{1}{2} \cdot m_3 \cdot \left(\dot{x}_{3d}(t)^2 + \dot{x}_{3q}(t)^2 \right) \\ PE_{dq}(t) = \dfrac{1}{2} \cdot k_{eq_1} \cdot \left(x_{1d}(t)^2 + x_{1q}(t)^2 \right) + \\ \quad + \dfrac{1}{2} \cdot k_{eq_2} \cdot \left(x_{2d}(t)^2 + x_{2q}(t)^2 \right) + \\ \quad + \dfrac{1}{2} \cdot k_{eq_3} \cdot \left(x_{3d}(t)^2 + x_{3q}(t)^2 \right) - \\ \quad -k_2 \cdot \left(x_{1d}(t) \cdot x_{2d}(t) + x_{1q}(t) \cdot x_{2q}(t) \right) - \\ \quad -k_3 \cdot \left(x_{2d}(t) \cdot x_{3d}(t) + x_{2q}(t) \cdot x_{3q}(t) \right) \\ \quad + \dfrac{1}{2} \cdot k_{eq_2} \cdot \left(x_{2d}(t)^2 + x_{2q}(t)^2 \right) \\ DE_{dq}(t) = \dfrac{1}{2} \cdot b_{eq_1} \cdot \left(\dot{x}_{1d}(t)^2 + \dot{x}_{1q}(t)^2 \right) + \\ \quad + \dfrac{1}{2} \cdot b_{eq_2} \cdot \left(\dot{x}_{2d}(t)^2 + \dot{x}_{2q}(t)^2 \right) + \\ \quad + \dfrac{1}{2} \cdot b_{eq_3} \cdot \left(\dot{x}_{2d}(t)^2 + \dot{x}_{2q}(t)^2 \right) + \\ \quad -b_2 \cdot \left(\dot{x}_{1d}(t) \cdot \dot{x}_{2d}(t) + \dot{x}_{1q}(t) \cdot \dot{x}_{2q}(t) \right) - \\ \quad -b_3 \cdot \left(\dot{x}_{2d}(t) \cdot \dot{x}_{3d}(t) + \dot{x}_{2q}(t) \cdot \dot{x}_{3q}(t) \right) \end{cases} \quad (42)$$

is necessary to obtain the mathematical expressions of each of these variables, through the solution of the dynamic models (based on the equations of motion). The primary goal of this section is to understand the mathematical structures for each variable and compare them with the simulation results. In addition, the mathematical structures of each variable will be presented.

A. Solution for 1-DoF in mechanical coordinates

The dynamic equation of motion (EoM) for the 1-DoF system is defined by (17). The EoM is redefined as follows

$$m_1 \cdot \ddot{x}_1(t) + b_{eq1} \cdot \dot{x}_1(t) + k_{eq1} \cdot x_1(t) = \\ = F \cdot \sin(\omega \cdot t) \quad (43)$$

where $x_1(t)$ and the parameters are defined in subsection III. The solution method (43) involves obtaining the general and particular solutions of (43) and then summing them to obtain the complete solution of the system [40], [41].

According to [40], [41], the complementary solution is based on the solution of the following unforced equation

$$m_1 \cdot \ddot{x}_{1c}(t) + b_{eq1} \cdot \dot{x}_{1c}(t) + k_{eq1} \cdot x_{1c}(t) = 0 \quad (44)$$

where $x_{1c}(t)$ is the complementary component of $x_1(t)$. where $x_{1c}(t)$ is the complementary component of $x_1(t)$. By using the change of the variable $x_{1c}(t) = e^{(D \cdot t)}$, where D is an arbitrary constant, and after applying it in (44), results

$$\left(m_1 \cdot D^2 + b_{eq1} \cdot D + k_{eq1}\right) \cdot e^{D \cdot t} = 0 \quad (45)$$

Solving (45) gives the solutions $D_1 = -\alpha + j \cdot \zeta$ and $D_2 = -\alpha - j \cdot \zeta$. Then, it is known that the solution for $x_{1c}(t)$, according to D_1 and D_2 [40] is described as

$$x_{1c}(t) = C_1 \cdot e^{-(\alpha - j \cdot \zeta) \cdot t} + C_2 \cdot e^{-(\alpha + j \cdot \zeta) \cdot t} \quad (46)$$

where C_1 and C_2 are typical integration constants that can be calculated considering the initial conditions of the system [40], [41]. According to the Euler equation [42] and trigonometric identities, the expression in (46) can be rewritten as

$$x_{1c}(t) = e^{-\alpha \cdot t} \cdot (X_1 \cdot \cos(\zeta \cdot t) + X_2 \cdot \sin(\zeta \cdot t)) \quad (47)$$

where $X_1 = C_1 + C_2$ and $X_2 = j \cdot (C_1 - C_2)$.

The particular solution of (43) is obtained by using the method of indeterminate coefficients [40]. This method is well suited to (43) because it involves a polynomial of the form $\sin(\omega t)$. Assuming a possible particular component of $x_1(t)$, i.e., $x_{1p}(t) = A \cdot \cos(\omega t) + B \cdot \sin(\omega t)$, one can compute $\dot{x}_{1p}(t) = -A \cdot \omega \cdot \sin(\omega \cdot t) + B \cdot \omega \cdot \cos(\omega \cdot t)$, and $\ddot{x}_{1p}(t) = -A \cdot \omega^2 \cdot \sin(\omega \cdot t) - B \cdot \omega^2 \cdot \cos(\omega \cdot t)$, where A and B are coefficients to be determined. To calculate A and B, these expressions ($x_{1p}(t)$, $\dot{x}_{1p}(t)$, and $\ddot{x}_{1p}(t)$) are replaced in (43) and by equating the trigonometric functions of the same type

present, a system of equations as a function of A and B is generated, such a system is shown as follows

$$\begin{bmatrix} k_{eq_1} - \omega^2 \cdot m_1 & \omega \cdot b_{eq_1} \\ -\omega \cdot b_{eq_1} & k_{eq_1} - \omega^2 \cdot m_1 \end{bmatrix} \cdot \begin{bmatrix} A \\ B \end{bmatrix} = \begin{bmatrix} 0 \\ F \end{bmatrix} \quad (48)$$

The expressions A and B are defined by

$$\begin{cases} A = -\dfrac{F \cdot \omega \cdot b_{eq_1}}{\left(k_{eq_1} - \omega^2 \cdot m_1\right) + \left(\omega \cdot b_{eq_1}\right)^2} \\ B = -\dfrac{F \cdot \left(k_{eq_1} - \omega^2 \cdot m_1\right)}{\left(k_{eq_1} - \omega^2 \cdot m_1\right) + \left(\omega \cdot b_{eq_1}\right)^2} \end{cases} \quad (49)$$

Applying trigonometric identities to $x_{1c}(t)$ and $x_{1p}(t)$, the complete solution of $x_1(t)$ is defined as follows

$$x_1(t) = x_{1c}(t) + x_{1p}(t) = \\ = e^{-\alpha \cdot t} \cdot X \cdot \sin(\zeta \cdot t + \rho) + T \cdot \sin(\omega \cdot t + \phi) \quad (50)$$

Here, $X = \text{sqrt}(X_1^2 + X_2^2)$, $\rho = \text{atan}(X_1/X_2)$, $T = \text{sqrt}(A^2 + B^2)$, and $\phi = \text{atan}(A/B)$.

B. Solution for 1-DoF in dq coordinates

The EoM in dq coordinates for this system is defined in (23). As in the previous case, i.e. the EoM in mechanical coordinates, the change in the variable $q_{1d}(t) = q_{2q}(t) = q_{2d}(t) = q_{2q}(t) = q_{2q}(t) = e^{(D \cdot t)}$ is used. Then, by replacing these variables in (23), the model of the system in function D is derived, which is defined by

$$\begin{bmatrix} D & -\omega & -1 & 0 \\ \omega & D & 0 & -1 \\ \dfrac{k_{eq_1}}{m_1} & 0 & D + \dfrac{b_{eq_1}}{m_1} & -\omega \\ 0 & \dfrac{k_{eq_1}}{m_1} & \omega & D + \dfrac{b_{eq_1}}{m_1} \end{bmatrix} \cdot \begin{bmatrix} q_{1_d}(t) \\ q_{1_q}(t) \\ q_{2_d}(t) \\ q_{2_q}(t) \end{bmatrix} = \\ = \begin{bmatrix} 0 \\ 0 \\ \dfrac{u_{1_d}(t)}{m_1} \\ \dfrac{u_{1_q}(t)}{m_1} \end{bmatrix} \quad (51)$$

Here, where $u_{1d}(t)$ and $u_{1q}(t)$ are the channels d and q of the input force to the transformed system (see section III).

Solving (51), the unforced equation of the system is obtained, which allows to obtain the complementary solutions and is defined by

$$\left(m_1^2 \cdot D^4 + 2 \cdot b_{eq1} \cdot m_1 \cdot D^3 + \\ + \left(b_{eq1}^2 + 2 \cdot m_1 \cdot \omega^2 + 2 \cdot k_{eq1} \cdot m_1\right) \cdot D^2 + \\ + \left(2 \cdot b_{eq1} \cdot m_1 \cdot \omega^2 + 2 \cdot b_{eq1} \cdot k_{eq1}\right) \cdot D + \\ + b_{eq1}^2 \cdot \omega^2 + k_{eq1}^2 - 2 \cdot k_{eq1} \cdot m_1 \cdot \omega^2 + \right. \quad (52)$$

$$+m_1{}^2 \cdot \omega^4) \cdot e^{D \cdot t} = 0$$

Solving (52), the solutions of D are defined in (53).

$$
\begin{cases}
D_1 = -\dfrac{1}{2} \cdot \left(\dfrac{b_{\mathrm{eq}_1} + \mathrm{j} \cdot \Gamma_1}{m_1}\right) \\[2mm]
D_2 = -\dfrac{1}{2} \cdot \left(\dfrac{b_{\mathrm{eq}_1} + \mathrm{j} \cdot \Gamma_2}{m_1}\right) \\[2mm]
D_3 = -\dfrac{1}{2} \cdot \left(\dfrac{b_{\mathrm{eq}_1} - \mathrm{j} \cdot \Gamma_1}{m_1}\right) \\[2mm]
D_4 = -\dfrac{1}{2} \cdot \left(\dfrac{b_{\mathrm{eq}_1} - \mathrm{j} \cdot \Gamma_2}{m_1}\right)
\end{cases}
\tag{53}
$$

The definitions of Γ_1 and Γ_2 can be expressed as follows

$$
\begin{cases}
\Gamma_1 = 2 \cdot \left(k_{\mathrm{eq}_1} \cdot m_1 + m_1{}^2 \cdot \omega^2 - \left(\dfrac{1}{2} \cdot b_{\mathrm{eq}_1}\right)^2 + \right. \\[2mm]
\left. + \mathrm{j} \cdot m_1 \cdot \omega \cdot \sqrt{b_{\mathrm{eq}_1}{}^2 - 4 \cdot k_{\mathrm{eq}_1} \cdot m_1}\right)^{\frac{1}{2}} \\[3mm]
\Gamma_2 = 2 \cdot \left(k_{\mathrm{eq}_1} \cdot m_1 + m_1{}^2 \cdot \omega^2 - \left(\dfrac{1}{2} \cdot b_{\mathrm{eq}_1}\right)^2 - \right. \\[2mm]
\left. - \mathrm{j} \cdot m_1 \cdot \omega \cdot \sqrt{b_{\mathrm{eq}_1}{}^2 - 4 \cdot k_{\mathrm{eq}_1} \cdot m_1}\right)^{\frac{1}{2}}
\end{cases}
\tag{54}
$$

Then the solutions for $q_{ijc}(t)$, where $i \in \{1,2\}$ and $j \in \{d, q\}$, have the form given by

$$
q_{ij_c}(t) = C_1 \cdot e^{-D_1 \cdot t} + C_2 \cdot e^{-D_2 \cdot t} + \\
+ C_3 \cdot e^{-D_3 \cdot t} + C_4 \cdot e^{-D_4 \cdot t}
\tag{55}
$$

Here, C_n where $n \in \{1, 2, 3, 4\}$ are integration constants that can be calculated considering the initial conditions of the system. Using the Euler equation and trigonometric identities, the expression in (55) can be rewritten in a new version defined by

$$
q_{ij_c}(t) = e^{-\alpha_{\mathrm{dq}} \cdot t} \cdot \left(X_{1_{\mathrm{dq}}} \cdot \cos\left(\zeta_{1_{\mathrm{dq}}} \cdot t + \rho_{1_{\mathrm{dq}}}\right) + \\
+ X_{2_{\mathrm{dq}}} \cdot \sin\left(\zeta_{2_{\mathrm{dq}}} \cdot t + \rho_{2_{\mathrm{dq}}}\right)\right)
\tag{56}
$$

To obtain the particular solution of (23), the method for solving systems of linear differential equations with constant coefficients given in [41] is used.

The first particular solution to be obtained is $q_{1\mathrm{dp}}(t)$, where the primitive equation is derived from the solution of (51) and from the consideration of D_n for $n \in \{1, 2, 3, 4\}$, which is defined as follows:

$$
q_{1_{\mathrm{dp}}}(t) = \prod_{i=1}^{4} \frac{1}{D + D_i} \cdot F \cdot b_{\mathrm{eq}_1} \cdot \omega
\tag{57}
$$

Then the following variable change is applied

$$
v_1(t) = \frac{1}{D + D_4} \cdot F \cdot b_{\mathrm{eq}_1} \cdot \omega \Rightarrow \frac{dv_1(t)}{dt} + \\
+ D_4 \cdot v_1(t) = F \cdot b_{\mathrm{eq}_1} \cdot \omega
\tag{58}
$$

where it can be verified that D works as a derivative operator $D = d/dt$. Solving the trivial linear difference equation in (58) gives the solution V_1, which is a constant, i.e

$$
V_1 = -2 \cdot \left(\frac{F \cdot b_{\mathrm{eq}_1} \cdot \omega \cdot m_1}{b_{\mathrm{eq}_1} - \mathrm{j} \cdot \Gamma_2}\right)
\tag{59}
$$

Now apply the following change of variable

$$
v_2(t) = \frac{1}{D + D_3} \cdot V_1 \Rightarrow \frac{dv_2(t)}{dt} + D_3 \cdot v_2(t) = V_1
\tag{60}
$$

Solving (60) gives

$$
V_2 = 4 \cdot \left(\frac{F \cdot b_{\mathrm{eq}_1} \cdot \omega \cdot m_1{}^2}{\left(b_{\mathrm{eq}_1} - \mathrm{j} \cdot \Gamma_1\right) \cdot \left(b_{\mathrm{eq}_1} - \mathrm{j} \cdot \Gamma_2\right)}\right)
\tag{61}
$$

Applying again the following change of variable

$$
v_3(t) = \frac{1}{D + D_2} \cdot V_2 \Rightarrow \frac{dv_3(t)}{dt} + D_2 \cdot v_3(t) = V_2
\tag{62}
$$

and solving (62), it gives

$$
V_3 = -4 \cdot \left(\frac{F \cdot b_{\mathrm{eq}_1} \cdot \omega \cdot m_1{}^3}{\left(b_{\mathrm{eq}_1} - \mathrm{j} \cdot \Gamma_1\right) \cdot \left(b_{\mathrm{eq}_1}{}^2 + \Gamma_2{}^2\right)}\right)
\tag{63}
$$

Finally, the fourth and final variable change required to achieve the particular solution is defined

$$
v_4(t) = \frac{1}{D + D_1} \cdot V_3 \Rightarrow \frac{dv_4(t)}{dt} + D_1 \cdot v_4(t) = V_3
\tag{64}
$$

whose solution is given by

$$
q_{1_{\mathrm{dp}}}(t) = V_4 = \\
= 16 \cdot \left(\frac{F \cdot b_{\mathrm{eq}_1} \cdot \omega \cdot m_1{}^4}{\left(b_{\mathrm{eq}_1}{}^2 + \Gamma_1{}^2\right) \cdot \left(b_{\mathrm{eq}_1}{}^2 + \Gamma_2{}^2\right)}\right)
\tag{65}
$$

The complete solution of $q_{1\mathrm{d}}(t)$ is given by:

$$
q_{1_{\mathrm{d}}}(t) = q_{1_{\mathrm{dc}}}(t) + q_{1_{\mathrm{dp}}}(t) = \\
= e^{-\alpha_{\mathrm{dq}} \cdot t} \cdot \left(X_{1_{\mathrm{dq}}} \cdot \cos\left(\zeta_{1_{\mathrm{dq}}} \cdot t + \rho_{1_{\mathrm{dq}}}\right) + \\
+ X_{2_{\mathrm{dq}}} \cdot \sin\left(\zeta_{2_{\mathrm{dq}}} \cdot t + \rho_{2_{\mathrm{dq}}}\right)\right) +
\tag{66}
$$

$$+16 \cdot \left(\frac{F \cdot b_{eq_1} \cdot \omega \cdot m_1{}^4}{\left(b_{eq_1}{}^2 + \Gamma_1{}^2\right) \cdot \left(b_{eq_1}{}^2 + \Gamma_2{}^2\right)} \right)$$

where $q_{1dc}(t)$ was already calculated and defined by (56).

Taking into account the procedure for solving the variable $q_{1d}(t)$ described by (57)–(66), the expressions for the remaining variables of the system in dq coordinates, i.e. $q_{1q}(t)$, $q_{2d}(t)$, and $q_{2q}(t)$, are derived and shown as follows

$$
\begin{aligned}
q_{1q}(t) = {}& e^{-\alpha_{dq} \cdot t} \cdot \left(X_{1_{dq}} \cdot \cos\left(\zeta_{1_{dq}} \cdot t + \rho_{1_{dq}}\right) + \right. \\
& \left. + X_{2_{dq}} \cdot \sin\left(\zeta_{2_{dq}} \cdot t + \rho_{2_{dq}}\right) \right) + \\
& + 16 \cdot \left(\frac{F \cdot \left(k_{eq_1} - m_1 \cdot \omega^2\right) \cdot m_1{}^4}{\left(b_{eq_1}{}^2 + \Gamma_1{}^2\right) \cdot \left(b_{eq_1}{}^2 + \Gamma_2{}^2\right)} \right)
\end{aligned}
\tag{67}
$$

$$
\begin{aligned}
q_{2d}(t) = {}& e^{-\alpha_{dq} \cdot t} \cdot \left(X_{1_{dq}} \cdot \cos\left(\zeta_{1_{dq}} \cdot t + \rho_{1_{dq}}\right) + \right. \\
& \left. + X_{2_{dq}} \cdot \sin\left(\zeta_{2_{dq}} \cdot t + \rho_{2_{dq}}\right) \right) + \\
& + 16 \cdot \left(\frac{F \cdot \omega \cdot \left(k_{eq_1} - m_1 \cdot \omega^2\right) \cdot m_1{}^4}{\left(b_{eq_1}{}^2 + \Gamma_1{}^2\right) \cdot \left(b_{eq_1}{}^2 + \Gamma_2{}^2\right)} \right)
\end{aligned}
\tag{68}
$$

$$
\begin{aligned}
q_{2q}(t) = {}& e^{-\alpha_{dq} \cdot t} \cdot \left(X_{1_{dq}} \cdot \cos\left(\zeta_{1_{dq}} \cdot t + \rho_{1_{dq}}\right) + \right. \\
& \left. + X_{2_{dq}} \cdot \sin\left(\zeta_{2_{dq}} \cdot t + \rho_{2_{dq}}\right) \right) + \\
& + 16 \cdot \left(\frac{F + \omega^2 \cdot m_1{}^4 \cdot b_{eq_1}}{\left(b_{eq_1}{}^2 + \Gamma_1{}^2\right) \cdot \left(b_{eq_1}{}^2 + \Gamma_2{}^2\right)} \right)
\end{aligned}
\tag{69}
$$

C. Solution for 2-DoF in mechanical coordinates

The 2-DoF system in mechanical coordinates is characterized using (17) and (25). However, it is more practical to represent the EoMs of this system as follows, i.e

$$
\begin{cases}
m_1 \cdot \ddot{x}_1(t) + b_{eq_1} \cdot \dot{x}_1(t) + k_{eq_1} \cdot x_1(t) - \\
\quad - b_2 \cdot \dot{x}_2(t) - k_2 \cdot x_2(t) = 0 \\
m_2 \cdot \ddot{x}_2(t) + b_{eq_2} \cdot \dot{x}_2(t) + k_{eq_2} \cdot x_2(t) - \\
\quad - b_2 \cdot \dot{x}_1(t) - k_2 \cdot x_1(t) = F \cdot \sin(\omega \cdot t)
\end{cases}
\tag{70}
$$

Use the same procedure presented in the subsection labeled as: Solution for 1-DoF in mechanical coordinates, to obtain the solutions of $x_1(t)$ and $x_2(t)$ shown below

$$
\begin{cases}
x_1(t) = e^{-\alpha_1 \cdot t} \cdot X_1 \cdot \sin(\zeta_1 \cdot t + \rho_1) + \\
\quad + e^{-\alpha_2 \cdot t} \cdot X_2 \cdot \sin(\zeta_2 \cdot t + \rho_2) + \\
\quad\quad + T_1 \cdot \sin(\omega \cdot t + \phi_1) \\
x_2(t) = e^{-\alpha_1 \cdot t} \cdot X_1 \cdot \sin(\zeta_1 \cdot t + \rho_1) + \\
\quad + e^{-\alpha_2 \cdot t} \cdot X_2 \cdot \sin(\zeta_2 \cdot t + \rho_2) + \\
\quad\quad + T_2 \cdot \sin(\omega \cdot t + \phi_2)
\end{cases}
\tag{71}
$$

where α_i, X_i, ζ_i, ρ_i, T_i, ϕ_i ($i \in \{1, 2\}$) are defined as follows: $\alpha_i = p_{i1}$, $X_i = \text{sqrt}(A_i{}^2 + B_i{}^2)$, $\zeta_i = p_{i2}$, $\rho_i = \text{atan}(A_i/B_{i2})$, $T_i = \text{sqrt}(A'_i{}^2 + B'_i{}^2)$, and $\phi_i = \text{atan}(B'_i/A'_i)$. The parameters A'_i and B'_i can be obtained by solving the system of equations in (72). Here, where **M**s are defined in (73). On the other hand, p_{i1} and p_{i2} correspond to the constants of the solutions of the D operators

$$
\begin{bmatrix} \mathbf{M_{11}} & \mathbf{M_{12}} \\ \mathbf{M_{21}} & \mathbf{M_{22}} \end{bmatrix} \cdot \begin{bmatrix} A'_1 \\ B'_1 \\ A'_2 \\ B'_2 \end{bmatrix} = \begin{bmatrix} F \cdot k_2 \\ F \cdot b_2 \cdot \omega \\ F \cdot \left(k_{eq_1} - \omega^2 \cdot b_2\right) \\ F \cdot b_{eq_1} \cdot \omega \end{bmatrix}
\tag{72}
$$

$$
\mathbf{M_{11}} = \begin{bmatrix} k_{eq_1} - \omega^2 \cdot m_1 & -\omega \cdot b_{eq_1} \\ \omega \cdot b_{eq_1} & k_{eq_1} - \omega^2 \cdot m_1 \end{bmatrix}
$$

$$
\mathbf{M_{12}} = \begin{bmatrix} k_2 & \omega \cdot b_2 \\ -\omega \cdot b_2 & -k_2 \end{bmatrix}
$$

$$
\mathbf{M_{21}} = \begin{bmatrix} -k_2 & \omega \cdot b_2 \\ -b_2 & -k_2 \end{bmatrix}
$$

$$
\mathbf{M_{22}} = \begin{bmatrix} k_{eq_2} - \omega^2 \cdot m_2 & -\omega \cdot b_{eq_2} \\ \omega \cdot b_{eq_2} & k_{eq_2} - \omega^2 \cdot m_2 \end{bmatrix}
\tag{73}
$$

as calculated in the 1-DoF case. It is verified that the solutions of D are defined as follows

$$
\begin{cases}
D_1 = -p_{11} + j \cdot p_{12} \\
D_2 = -p_{11} - j \cdot p_{12} \\
D_3 = -p_{21} + j \cdot p_{22} \\
D_4 = -p_{21} - j \cdot p_{22}
\end{cases}
\tag{74}
$$

Due to the length of the expressions of p_{i1} and p_{i2}, in this article they will be referred to only as those mentioned above, instead of the exact expressions.

Finally, A_i and B_i are defined as $A_1 = C_{11} + C_{12}$, $B_1 = j \cdot (C_{11} - C_{12})$, $A_2 = C_{13} + C_{14}$, and $B_2 = j \cdot (C_{13} - C_{14})$, where C_{1n} ($n \in \{1, 2, 3, 4\}$) are integration constants which must be calculate them taking into account initial conditions.

D. Solution for 2-DoF in dq coordinates

The model in dq coordinates is defined in (23). Then, following the same procedure developed in the subsection Solution for 1-DoF in dq coordinates, the solutions of the variables $q_{ij}(t)$, where $i \in \{1, 2, 3, 4\}$ and $j \in \{d, q\}$, are defined as

$$
q_{i_j}(t) = \sum_{i=1}^{4} \left[e^{-\alpha_{i_{dq}} \cdot t} \cdot X_{i_{dq}} \cdot \sin\left(\zeta_{i_{dq}} \cdot t + \rho_{i_{dq}}\right) + \frac{\dfrac{k_i}{d}}{\prod_{i=0}^{4}(p_{i1}{}^2 + p_{i2}{}^2)} \right]
\tag{75}
$$

In this system, it can be verified that the solutions for D can be determined as

$$
\begin{cases}
D_1 = -p_{11} + j \cdot p_{12} \\
D_2 = -p_{11} - j \cdot p_{12} \\
D_3 = -p_{21} + j \cdot p_{22} \\
D_4 = -p_{21} - j \cdot p_{22} \\
D_5 = -p_{31} + j \cdot p_{32} \\
D_6 = -p_{31} - j \cdot p_{32} \\
D_7 = -p_{41} + j \cdot p_{42} \\
D_8 = -p_{41} - j \cdot p_{42}
\end{cases}
\tag{76}
$$

Therefore, $\alpha_{idq} = \Re e\{D_n\}$ $\zeta_{idq} = \Im m\{D_n\}$, where $n \in \{1, 3, 5, 7\}$. Also, $\rho_i = \text{atan}(A_i/B_i)$ and $X_{idq} = \text{sqrt}(A_i^2 + B_i^2)$. Finally, $A_i = C_{1h} + C_{1(h+1)}$ and $B_i = C_{1h} - C_{1(h+1)}$ for $h \in \{1, 2, 3, 4, 5, 6, 7, 8\}$.

E. Solution for 3-DoF in mechanical coordinates

The EoMs that model this system are defined as

$$\begin{cases} m_1 \cdot \ddot{x}_1(t) + b_{eq_1} \cdot \dot{x}_1(t) + k_{eq_1} \cdot x_1(t) - \\ \quad -b_2 \cdot \dot{x}_2(t) - k_2 \cdot x_2(t) = 0 \\ m_2 \cdot \ddot{x}_2(t) + b_{eq_2} \cdot \dot{x}_2(t) + k_{eq_2} \cdot x_2(t) - \\ \quad -b_2 \cdot \dot{x}_1(t) - k_2 \cdot x_1(t) = 0 \\ m_3 \cdot \ddot{x}_3(t) + b_{eq_3} \cdot \dot{x}_3(t) + k_{eq_3} \cdot x_3(t) - \\ -b_3 \cdot \dot{x}_2(t) - k_3 \cdot x_2(t) = F \cdot \sin(\omega \cdot t) \end{cases} \quad (77)$$

Subsequently, the solutions for the 3-DoF system in mechanical coordinates can be derived and defined as follows

$$\begin{cases} x_1(t) = e^{-\alpha_1 \cdot t} \cdot X_1 \cdot \sin(\zeta_1 \cdot t + \rho_1) + \\ \quad e^{-\alpha_2 \cdot t} \cdot X_2 \cdot \sin(\zeta_2 \cdot t + \rho_2) + \\ +e^{-\alpha_3 \cdot t} \cdot X_3 \cdot \sin(\zeta_3 \cdot t + \rho_3) + T_1 \cdot \sin(\omega \cdot t + \phi_1) \\ x_2(t) = e^{-\alpha_1 \cdot t} \cdot X_1 \cdot \sin(\zeta_1 \cdot t + \rho_1) + \\ \quad +e^{-\alpha_2 \cdot t} \cdot X_2 \cdot \sin(\zeta_2 \cdot t + \rho_2) + \\ +e^{-\alpha_3 \cdot t} \cdot X_3 \cdot \sin(\zeta_3 \cdot t + \rho_3) + T_2 \cdot \sin(\omega \cdot t + \phi_2) \\ x_3(t) = e^{-\alpha_1 \cdot t} \cdot X_1 \cdot \sin(\zeta_1 \cdot t + \rho_1) + \\ \quad +e^{-\alpha_2 \cdot t} \cdot X_2 \cdot \sin(\zeta_2 \cdot t + \rho_2) + \\ +e^{-\alpha_3 \cdot t} \cdot X_3 \cdot \sin(\zeta_3 \cdot t + \rho_3) + T_3 \cdot \sin(\omega \cdot t + \phi_3) \end{cases} \quad (78)$$

where $X_i = \text{sqrt}(A_i^2 + B_i^2)$ and $\rho_i = \text{atan}(A_i/B_i)$ valid for $i \in \{1, 2, 3\}$. Also, A_i and B_i are defined as $A_1 = C_{11} + C_{12}$, $B_1 = \text{j} \cdot (C_{11} - C_{12})$, $A_2 = C_{13} + C_{14}$, $B_2 = \text{j} \cdot (C_{13} - C_{14})$, $A_3 = C_{15} + C_{16}$, and $B_3 = \text{j} \cdot (C_{15} - C_{16})$, where C_{1n} ($n \in \{1, 2, 3, 4, 5, 6\}$) are integration constants which must be calculate them taking into account initial conditions. On the other hand, $T_i = \text{sqrt}(A'^2_i + B'^2_i)$ and $\phi_i = \text{atan}(B'_i/A'_i)$. Similar to the 2-DoF system, the constants A'_i and B'_i are calculated via a system of equations, which are too lengthy to include in this article. When developing solutions for operator D, its definition is outlined below

$$\begin{cases} D_1 = -p_{11} + \text{j} \cdot p_{12} \\ D_2 = -p_{11} - \text{j} \cdot p_{12} \\ D_3 = -p_{21} + \text{j} \cdot p_{22} \\ D_4 = -p_{21} - \text{j} \cdot p_{22} \\ D_5 = -p_{31} + \text{j} \cdot p_{32} \\ D_6 = -p_{31} - \text{j} \cdot p_{32} \end{cases} \quad (79)$$

Therefore $\alpha_i = \Re e\{D_n\}$ $\zeta_i = \Im m\{D_n\}$, where $n \in \{1, 3, 5\}$.

F. Solution for 3-DoF in dq coordinates

The model of the 3-DoF system in dq coordinates is modeled by (23). The solution of this system is then defined in (80), where $i \in \{1, 2, 3, 4, 5\}$ and $j \in \{d, q\}$. In this system, it can be also verified that the solutions for D can be determined in (81). Therefore, $\alpha_{idq} = \Re e\{D_n\}$ $\zeta_{idq} = \Im m\{D_n\}$, where $n \in \{1, 3, 5, 7, 9\}$. Also, $\rho_i = \text{atan}(A_i/B_i)$ and $X_{idq} = \text{sqrt}(A_i^2 + B_i^2)$.

$$q_{i_j}(t) = \sum_{i=1}^{5} \left[e^{-\alpha_{i dq} \cdot t} \cdot X_{i_{dq}} \cdot \sin\left(\zeta_{i_{dq}} \cdot t + \rho_{i_{dq}}\right) + \right. \\ \left. + \frac{\dfrac{k_i}{d}}{\prod_{i=0}^{5}(p_{i1}^2 + p_{i2}^2)} \right] \quad (80)$$

$$\begin{cases} D_1 = -p_{11} + \text{j} \cdot p_{12} \\ D_2 = -p_{11} - \text{j} \cdot p_{12} \\ D_3 = -p_{21} + \text{j} \cdot p_{22} \\ D_4 = -p_{21} - \text{j} \cdot p_{22} \\ D_5 = -p_{31} + \text{j} \cdot p_{32} \\ D_6 = -p_{31} - \text{j} \cdot p_{32} \\ D_7 = -p_{41} + \text{j} \cdot p_{42} \\ D_8 = -p_{41} - \text{j} \cdot p_{42} \\ D_9 = -p_{51} + \text{j} \cdot p_{52} \\ D_{10} = -p_{51} - \text{j} \cdot p_{52} \end{cases} \quad (81)$$

Finally, $A_i = C_{1h} + C_{1(h+1)}$ and $B_i = C_{1h} - C_{1(h+1)}$ for $h \in \{1, 2, 3, 4, 5, 6, 7, 8, 9, 10\}$.

From the analysis made in this section, three fundamental aspects can be considered, namely

- Taking into account the solution procedure carried out to solve the systems in mechanical coordinates as well as in dq coordinates, and considering the linearity of these, one can easily extend the order of this type of vibrational system, obtaining the solutions, in both coordinates, for n-DoF.

- Regarding the solutions of the systems p-DoF ($p \in \{1, 2, 3\}$) in mechanical coordinates, it can be seen that the mathematical structure of these solutions is composed of two parts; one of them responds to a free or transient vibration, which is a periodic motion where it is observed how the system moves from its static equilibrium position; and the other part is the forced vibration that occurs when an external force − as in this study with the force $f(t)$ = $F \cdot \sin(\omega t)$ − acts on the system during its vibrational motion [43], [44]. It is obvious that at the time of forced vibration, the system will tend to vibrate at its own natural frequency and at the same time follow the frequency of the exerted force [43], [44].

- The mathematical structure of solutions for p-DoF systems in dq coordinates is constituted by two parts: a transient component and a constant component that prevails in time. It is worth noting that systems in dq coordinates exhibit this response pattern, as variables involved in temporal evolution are converted into variables displaying constant characteristics within this domain [25], [27]–[29].

VI. SIMULATION RESULTS

This section thoroughly examines the simulation results of the proposed 1-, 2-, and 3-DoF systems in both mechanical and

dq coordinates. All systems, including the 1-, 2-, and 3-DoF models, are uniformly affected by a sinusoidal force with an amplitude of 900 N and a linear frequency of 10 kHz. Table I outlines the specific simulation parameters for each system, maintaining standardized initial conditions where $x_{i0}(t) = dx_{i0}(t)/dt = 0$ for $i \in \{1, 2, 3\}$.

The simulation results for the 1-DoF system in mechanical coordinates are illustrated in Fig. 6, which provides a detailed view of the dynamics. Specifically, Fig. 6(a) and (b) show the behavior of the position variable, $x_1(t)$, and the velocity variable, $dx_1(t)/dt$, respectively. Furthermore, Fig. 6(c) and (d) provide a zoomed view of these variables. with a zoomed view. Fig. 6(d) emphasizes the dynamic behavior of the force acting on the system, denoted $f_1(t)$.

Moving the focus to the dq coordinates, Fig. 7 illustrates the transient simulation results of the 1-DoF system. Fig. 7(a)–(c) reveal the dynamics of the d and q channels with respect to $q_{1d}(t)$, $q_{1q}(t)$, $q_{2d}(t)$, $q_{2q}(t)$, and the excitation forces $f_{1d}(t)$ and $f_{1q}(t)$, respectively.

Analyzing Fig. 6(a), the amplitude of the forced vibration component is significantly smaller than the amplitude of the free vibration component, as expressed in (50), where T << X. On the other hand, one can verify the expression of $\dot{x}_1(t) = \sqrt{\alpha^2 + \zeta^2} \cdot X \cdot e^{-\alpha \cdot t} \cdot \cos\left(\zeta \cdot t + \rho + \tan^{-1}\left(\frac{\alpha}{\zeta}\right)\right) + \omega \cdot T \cdot \cdot \cos(\omega \cdot t + \phi)$ which is easily obtained from (50), by inspecting Fig. 6(b). Also, Fig. 6(b) shows the existence of both transient and steady state components of velocity, exemplified by the expression for $dx_1(t)/dt$. The frequency of the free vibration component is approximately $\zeta \approx 0.323$ rad/s, while the forced vibration component corresponds to a frequency of $\omega \approx 62.832 \cdot 10^3$ rad/s.

Focusing on the dynamics in dq coordinates shown in Fig. 7(a) and 7(b), one can observe a transient component with a cosine-type behavior and a steady-state component depicted as

TABLE I. PARAMETERS OF 1-, 2-, AND 3-DoF SYSTEM

System	Parameters	Values
1-DoF	k_1	10 N/m
	k_2	1 N/m
	b_1	$10 \cdot 10^{-1}$ N-s/m
	b_2	1.5 N-s/m
	m_1	100 kg
2-DoF	k_1	10 N/m
	k_2	1 N/m
	k_3	1.1 N/m
	b_1	10 N-s/m
	b_2	11 N-s/m
	b_3	1 N-s/m
	m_1	100 kg
	m_2	100 kg
3-DoF	k_1	10 N/m
	k_2	1 N/m
	k_3	11 N/m
	k_4	1.1 N/m
	b_1	1 N-s/m
	b_2	$1.1 \cdot 10^{-5}$ N-s/m
	b_3	$1 \cdot 10^{-6}$ N-s/m
	b_4	$10 \cdot 10^{-6}$ N-s/m
	m_1	100 kg
	m_2	100 kg
	m_3	100 kg

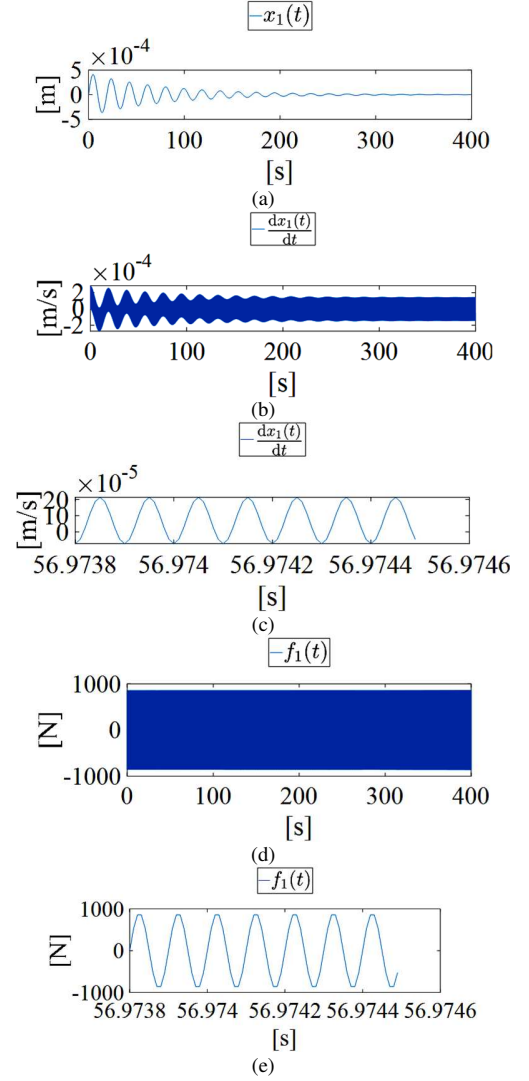Fig. 6. Under transient simulation results of the 1-DoF system in mechanical coordinates. Initial conditions $x_{10}(t) = dx_{10}(t)/dt = 0$. (a) Dynamics of $x_1(t)$. (b) Dynamics of $dx_1(t)/dt$. (c) Zoomed view of $x_1(t)$. (d) Dynamics of $f_1(t)$. (e) Zoomed view of $f_1(t)$.

constant, which agrees with (66)–(69). The excitation force conversion to dq produces d and q channels for each component. Specifically, the d component has a force of $f_{1d}(t) = 0$ N, and the q channel has a force of $f_{1q}(t) = 900$ N. Table II provides a summary of the steady-state values for the variables $q_{nm}(t)$, where $n \in \{1, 2\}$ and $m \in \{d, q\}$, as depicted in Fig. 7.

The transient dynamics of $x_1(t)$, $dx_1(t)/dt$, $x_2(t)$, and $dx_2(t)/dt$ for the mechanical coordinates of the 2-DoF system are depicted in Fig. 8. The expression of $x_1(t)$ is verified by Fig. 8(a). The dynamics exhibit two frequencies that correspond to transient components, as detailed in (71). Furthermore, the transient period features observable maxima, demonstrating a beating phenomenon [43], [44]. This can be expanded to $x_2(t)$ illustrated in Fig. 8(c), comprising of two components: a sub-frequency reaching 1.31 mHz, which represents the natural

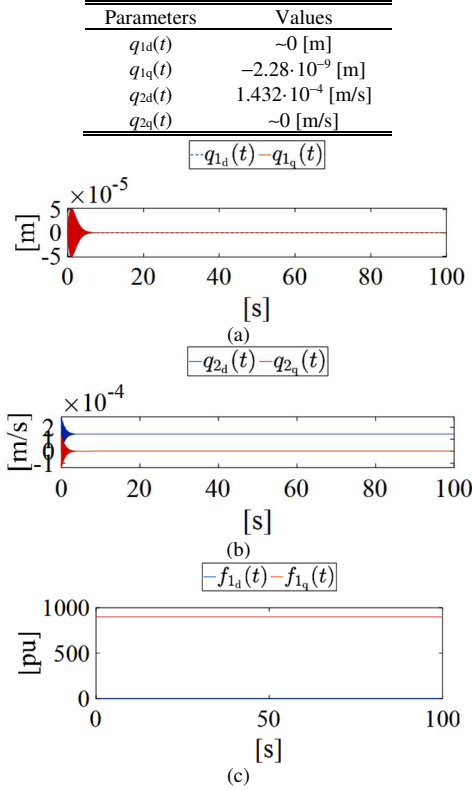| Parameters	Values
$q_{1d}(t)$	~0 [m]
$q_{1q}(t)$	$-2.28 \cdot 10^{-9}$ [m]
$q_{2d}(t)$	$1.432 \cdot 10^{-4}$ [m/s]
$q_{2q}(t)$	~0 [m/s]

Fig. 7. Under transient simulation results of the 1-DoF system in dq coordinates. Initial conditions $q_{mn}(t) = 0$ where $m \in \{1, 2\}$ and $n \in \{d, q\}$. (a) Dynamics of $q_{1d}(t)$ and $q_{1q}(t)$. (b) Dynamics of $q_{1d}(t)$ and $q_{1q}(t)$. (c) Dynamics of $f_{1d}(t)$ and $f_{1q}(t)$.

frequency, and a high-frequency component of 10 kHz from $f_1(t)$. Fig. 8(d) enhances the maxima and minima in the variables of the system, $x_i(t)$ and $dx_i(t)/dt$ for $i \in \{1, 2\}$, evidencing variations within the system's energies [43], [44].

The dynamics of the 2-DoF system in dq coordinates is elucidated in Fig. 9, with variables $q_{mn}(t)$, where $m \in \{1, 2, 3, 4\}$ and $n \in \{d, q\}$, as shown in Fig. 9(a)−(d). The $q_{mn}(t)$ variables exhibit two components, a transient regime, and a stationary regime, which are modeled in (75), similar to the 1-DoF system. Table III summarizes the steady-state values for both components, which are significantly close to zero.

Fig. 10 illustrates the mechanical coordinate dynamics of the 3-DoF system, showing the variables $x_1(t)$, $dx_1(t)/dt$, $x_2(t)$, $dx_2(t)/dt$, $x_3(t)$, and $dx_3(t)/dt$ for Fig. 10(a)−10(f). As in the 2-DoF system, $x_1(t)$ satisfies its expression, describing both a transient and a steady state component. Fig. 10(e) and (f) show the typical response of $dx_3(t)/dt$ of the body with mass m_3 when subjected to the excitation force ($f_1(t)$).

Fig. 11 illustrates the dynamics of variables in dq coordinates for the 3-DoF model, with a focus on $q_{mn}(t)$ variables, where $m \in \{1, 2, 3, 4, 5, 6\}$ and $n \in \{d, q\}$. Similar to the 2-DoF system, $q_{mn}(t)$ contains two components, namely transient and steady states, that have been verified by (80). The magnitudes of $q_{mn}(t)$ are negligible, as summarized in Table IV.
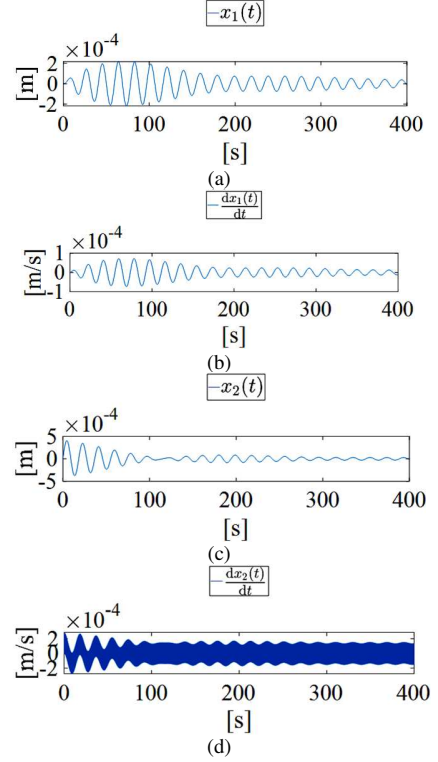

Fig. 8. Under transient simulation results of the 2-DoF system in mechanical coordinates. Initial conditions $x_{i0}(t) = dx_{i0}(t)/dt = 0$ where $i \in \{1, 2\}$. (a) Dynamics of $x_1(t)$. (b) Dynamics of $dx_1(t)/dt$. (c) Dynamics of $x_2(t)$. (d) Dynamics of $dx_2(t)/dt$.
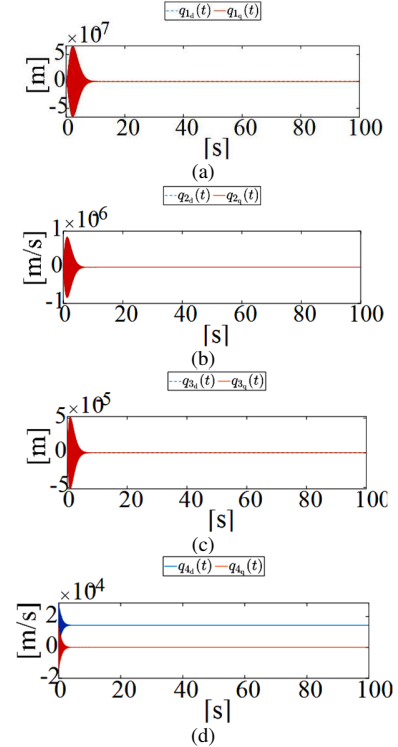

Fig. 9. Under transient simulation results of the 2-DoF system in dq coordinates. Initial conditions $q_{mn}(t) = 0$ where $m \in \{1, 2, 3, 4\}$ and $n \in \{d, q\}$. (a) Dynamics of $q_{1d}(t)$ and $q_{1q}(t)$. (b) Dynamics of $q_{2d}(t)$ and $q_{2q}(t)$. (c) Dynamics of $q_{3d}(t)$ and $q_{3q}(t)$. (d) Dynamics of $q_{4d}(t)$ and $q_{4q}(t)$.

TABLE III. 2-DoF STEADY-STATE VALUES OF $q_{nm}(t)$ $\forall$ $m \in \{1, 2, 3, 4\}$ AND n $\in \{d, q\}$

Parameters	Values	Parameters	Values
$q_{1d}(t)$	~0 [m]	$q_{3d}(t)$	~0 [m/s]
$q_{1q}(t)$	~0 [m]	$q_{3q}(t)$	~0 [m/s]
$q_{2d}(t)$	~0 [m/s]	$q_{4d}(t)$	$1.432 \cdot 10^{-4}$ [m/s]
$q_{2q}(t)$	~0 [m/s]	$q_{4q}(t)$	~0 [m/s]

TABLE IV. 3-DoF STEADY-STATE VALUES OF $q_{nm}(t)$ $\forall$ $m \in \{1, 2, 3, 4, 5, 6\}$ AND $n \in \{d, q\}$

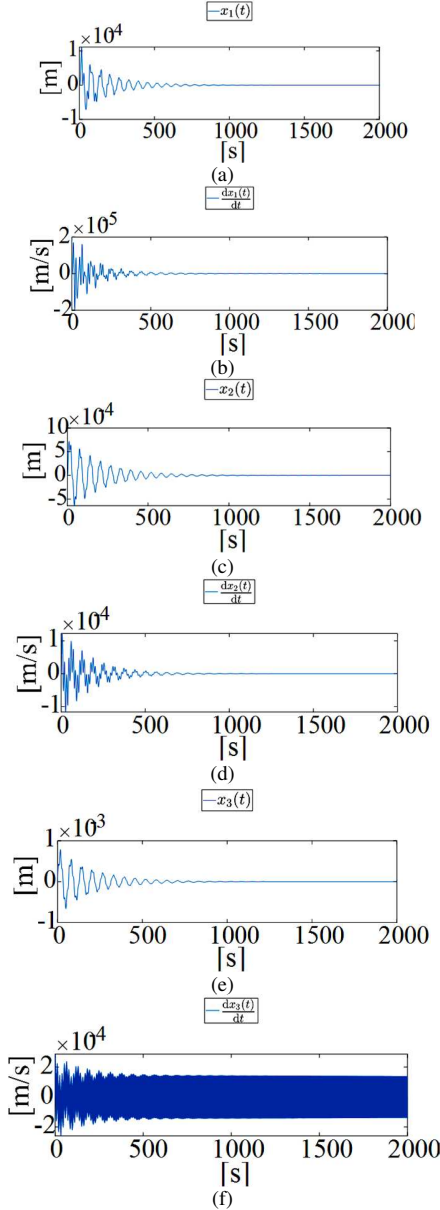| Parameters	Values	Parameters	Values
$q_{1d}(t)$	~0 [m]	$q_{4d}(t)$	~0 [m/s]
$q_{1q}(t)$	~0 [m]	$q_{4q}(t)$	~0 [m/s]
$q_{2d}(t)$	~0 [m/s]	$q_{5d}(t)$	~0 [m]
$q_{2q}(t)$	~0 [m/s]	$q_{5q}(t)$	$-2.28 \cdot 10^{-9}$ [m]
$q_{3d}(t)$	~0 [m]	$q_{6d}(t)$	$1.432 \cdot 10^{-4}$ [m/s]
$q_{3q}(t)$	~0 [m]	$q_{6q}(t)$	~0 [m/s]

Fig. 10. Under transient simulation results of the 3-DoF system in mechanical coordinates. Initial conditions $x_{i0}(t) = dx_{i0}(t)/dt = 0$ for $i \in \{1, 2, 3\}$. (a) Dynamics of $x_1(t)$. (b) Dynamics of $dx_1(t)/dt$. (c) Dynamics of $x_2(t)$. (d) Dynamics of $dx_2(t)/dt$. (e) Dynamics of $x_3(t)$. (f) Dynamics of $dx_3(t)/dt$.
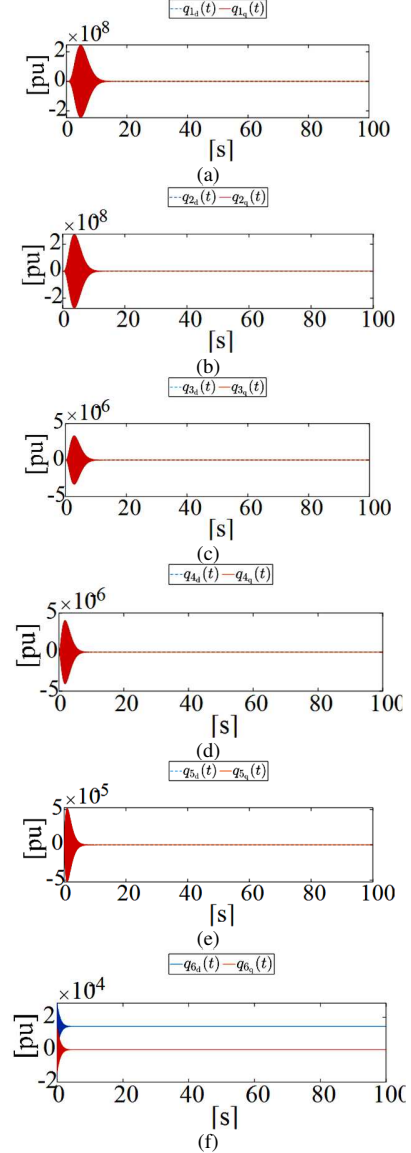

Fig. 11. Under transient simulation results of the 3-DoF system in dq coordinates. Initial conditions $q_{mn}(t) = 0$ where $m \in \{1, 2, 3, 4, 5, 6\}$ and $n \in \{d, q\}$. (a) Dynamics of $q_{1d}(t)$ and $q_{1q}(t)$. (b) Dynamics of $q_{2d}(t)$ and $q_{2q}(t)$. (c) Dynamics of $q_{3d}(t)$ and $q_{3q}(t)$. (e) Dynamics of $q_{5d}(t)$ and $q_{5q}(t)$. (f) Dynamics of $q_{6d}(t)$ and $q_{6q}(t)$

The dynamic responses of 1-, 2-, and 3-DOF systems using a sinusoidal force are carefully examined in this section. For the 1-DoF system, low damping results in an oscillatory pattern displaying dual frequency components. The conversion to dq coordinates simplifies the dynamics. The 2-DoF system presents complex interactions and highlights beating

phenomena and multi-frequency components. The dq coordinates underscore minimal contributions from masses unexposed to external forces. The 3-DoF system exhibits various interactions with two distinct frequency components. The dq transformation demonstrates efficacy and suggests a

focused analysis of externally influenced variables. In general, this section offers significant insights into system dynamics, directing future research towards streamlined analytical frameworks.

VII. Conclusion

In summary, conducting an in-depth simulation and subsequent analysis of the proposed single, dual, and triple degree-of-freedom mechanical systems subject to sinusoidal force has yielded comprehensive insights into their dynamic intricacies. The single degree-of-freedom system, distinguished by low damping, displays a fascinating oscillatory pattern characterized by dual frequency components. The conversion from spatial to dq coordinates provides a tactical reduction of the system's dynamics, illuminating its complex behavior. Moving towards the 2-degree-of-freedom system, greater levels of complexity are discernible within its mechanical coordinates, where elaborate interactions, beating phenomena, and the presence of multiple frequency components are noteworthy. The analysis in dq coordinates highlights the minimal influence of masses not subjected to external forces, emphasizing the usefulness of such transformations in revealing the underlying system dynamics.

The 3-degree-of-freedom system highlights the success of the dq transformation in illuminating externally influenced variables through its varied interactions and dual frequency components. A sinusoidal force produces variations in system energies, and the dynamic responses reveal the nuanced interplay between various components within the system. The thorough investigation of these systems not only enhances our comprehension of their operations but also underscores the significance of efficient analytical frameworks in deciphering complex dynamics.

Furthermore, the results of this study have extensive implications for the area of dynamic systems analysis. The observed oscillations, patterns of beating, and multiple frequencies present in various degrees of freedom provide valuable insight on how to refine analytical approaches and improve methods for studying dynamic systems. Standardized initial conditions and the impact of damping on the system's overall behavior further contribute to the study's robustness. In conclusion, this study enhances our comprehension of simulated systems and proposes fruitful areas for future inquiry, facilitating the creation of more precise analytical frameworks to explore externally influenced variables in dynamic mechanical systems further.

References

[1] D. Findeisen, *System Dynamics and Mechanical Vibrations: An Introduction*. 2010.

[2] R. Arias, A. P. da Cunha, and A. R. Garcia Ramirez, "Teaching of mechanical vibration concepts using the computational simulation," *IEEE Latin America Transactions*, vol. 18, no. 04, pp. 659–667, Apr. 2020.

[3] E. A. Burda, G. V. Zusman, I. S. Kudryavtseva, and A. P. Naumenko, "An Overview of Vibration Analysis Techniques for the Fault Diagnostics of Rolling Bearings in Machinery," *Shock and Vibration*, vol. 2022, p. e6136231, Dec. 2022.

[4] H. P. Bloch and F. K. Geitner, Eds., "Chapter 5 - Vibration Analysis," in *Practical Machinery Management for Process Plants*, vol. 2, Gulf Professional Publishing, 1999, pp. 351–433.

[5] B. Yang, "Chapter 10 - Vibration analysis of one-degree-of-freedom systems," in *Stress, Strain, and Structural Dynamics (Second Edition)*, B. Yang, Ed. Academic Press, 2023, pp. 431–528.

[6] F. Svaricek, C. Bohn, P. Marienfeld, H.-J. Karkosch, T. Fueger, F. Svaricek, C. Bohn, P. Marienfeld, H.-J. Karkosch, and T. Fueger, "Automotive Applications of Active Vibration Control," in *Vibration Control*, IntechOpen, 2010.

[7] O. I. Vulcu and M. Arghir, "Impact of maintenance in the automotive field. Experimental study of mechanical vibration," *IOP Conf. Ser.: Mater. Sci. Eng.*, vol. 147, no. 1, p. 012056, Aug. 2016.

[8] Z. You, "Design of automotive mechanical automatic transmission system based on torsional vibration reduction," *Journal of Vibroengineering*, vol. 25, no. 4, pp. 683–697, Jun. 2023.

[9] M. Bonato and P. Goge, "Methods for analysis and comparison of automotive vibration tests," in *2016 Annual Reliability and Maintainability Symposium (RAMS)*, pp. 1–6, Jan. 2016.

[10] K. C. Panda, "Dealing with Noise and Vibration in Automotive Industry," *Procedia Engineering*, vol. 144, pp. 1167–1174, Jan. 2016.

[11] S. Jiang, H. Liu, Z. Gu, and Q. Liu, "Mechanical Simulation Analysis of Aerospace High Reliability Electronic Equipment," *J. Phys.: Conf. Ser.*, vol. 2187, no. 1, p. 012035, Feb. 2022.

[12] L. Liu and B. Tian, "Comprehensive Engineering Frequency Domain Analysis and Vibration Suppression of Flexible Aircraft Based on Active Disturbance Rejection Controller," *Sensors*, vol. 22, no. 16, p. 6207, Jan. 2022.

[13] B. A and S. Zolkiewski, "Dynamic analysis of the mechanical systems vibrating transversally in transportation," *Journal of Achievements in Materials and Manufacturing Engineering*, vol. 20, Jan. 2007.

[14] W. Wang, G. Shen, Y. Zhang, Z. Zhu, C. Li, and H. Lu, "Dynamic reliability analysis of mechanical system with wear and vibration failure modes," *Mechanism and Machine Theory*, vol. 163, p. 104385, Sep. 2021.

[15] K. Kamei and M. A. Khan, "Current challenges in modelling vibrational fatigue and fracture of structures: a review," *J Braz. Soc. Mech. Sci. Eng.*, vol. 43, no. 2, p. 77, Jan. 2021.

[16] M. Romanssini, P. C. C. de Aguirre, L. Compassi-Severo, and A. G. Girardi, "A Review on Vibration Monitoring Techniques for Predictive Maintenance of Rotating Machinery," *Eng*, vol. 4, no. 3, pp. 1797–1817, Sep. 2023.

[17] D. Y. Ou and C. M. Mak, "A Review of Prediction Methods for the Transient Vibration and Sound Radiation of Plates," *Journal of Low Frequency Noise, Vibration and Active Control*, vol. 32, no. 4, pp. 309–322, Dec. 2013.

[18] N. Anh and N. Nguyen, "Design of non-traditional dynamic vibration absorber for damped linear structures," *Proceedings of the Institution of Mechanical Engineers, Part C: Journal of Mechanical Engineering Science*, vol. 228, no. 1, pp. 45–55, Jan. 2014.

[19] M. H. Mohd Ghazali and W. Rahiman, "Vibration Analysis for Machine Monitoring and Diagnosis: A Systematic Review," *Shock and Vibration*, vol. 2021, p. e9469318, Sep. 2021.

[20] S. Saxena and M. Patel, "Evaluating dynamic behavior of a concrete dam using modal analysis," *Materials Today: Proceedings*, Aug. 2023.

[21] H. Van der Auweraer, "Structural dynamics modeling using modal analysis: applications, trends and challenges," in *IMTC 2001. Proceedings of the 18th IEEE Instrumentation and Measurement Technology Conference. Rediscovering Measurement in the Age of Informatics (Cat. No.01CH 37188)*, vol. 3, pp. 1502–1509 vol.3, May 2001.

[22] K. Ogata, *Modern Control Engineering*, 5th edition. Boston: Pearson, 2009.

[23] B. C. Kuo, *Automatic control systems*, 6th edition. Englewood Cliffs, N.J: Prentice Hall, 1991.

[24] W. S. Levine, *The Control Handbook (three volume set)*. CRC Press, 2018.

[25] C. J. O'Rourke, M. M. Qasim, M. R. Overlin, and J. L. Kirtley Jr, "A Geometric Interpretation of Reference Frames and Transformations: dq0, Clarke, and Park," *Colm O'Rourke*, Dec. 2019.

[26] M. Gonzalez, V. Cardenas, and F. Pazos, "DQ transformation development for single-phase systems to compensate harmonic distortion and reactive power," in *9th IEEE International Power Electronics Congress, 2004. CIEP 2004*, pp. 177–182, Oct. 2004.

[27] M. F. Schonardie and D. C. Martins, "Application of the dq0 transformation in the three-phase grid-connected PV systems with active and reactive power control," in *2008 IEEE International Conference on Sustainable Energy Technologies*, pp. 18–23, Nov. 2008.

[28] K. S. Low, M. F. Rahman, and K. W. Lim, "The dq transformation and feedback linearization of a permanent magnet synchronous motor," in *Proceedings of 1995 International Conference on Power Electronics and Drive Systems. PEDS 95*, pp. 292–296 vol.1, Feb. 1995.

[29] S. W. L. Tobing, R. Afdila, P. E. Panjaitan, N. C. Situmeang, K. N. Hutagalung, and R. Sidabutar, "ABC to DQ Transformation for Three-Phase Inverter Design as Prime Mover Speed Control in Microgrid System," in *2022 6th International Conference on Electrical, Telecommunication and Computer Engineering (ELTICOM)*, pp. 70–74, Nov. 2022.

[30] M. F. Schonardie, R. F. Coelho, R. Schweitzer, and D. C. Martins, "Control of the active and reactive power using dq0 transformation in a three-phase grid-connected PV system," in *2012 IEEE International Symposium on Industrial Electronics*, pp. 264–269, May 2012.

[31] K. Abe, *The Clark and Park transformations: Coordinate transformations for Brushless DC motor in field-oriented control*.

[32] B. C. Trento, "Modeling and Control of Single Phase Grid-Tie Converters," *Masters Theses*, Aug. 2012.

[33] A. C. J. Luo, *Nonlinear Deformable-body Dynamics*, 2010th edition. Beijing : Berlin ; New York: Springer Verlag, 2010.

[34] A. W. Pila, *Introduction to Lagrangian Dynamics*, 1st ed. 2020 edition. Cham, Switzerland: Springer, 2019.

[35] G. A. Anastassiou and I. F. Iatan, "Linear Transformations," in *Intelligent Routines II: Solving Linear Algebra and Differential Geometry with Sage*, G. A. Anastassiou and I. F. Iatan, Eds. Cham: Springer International Publishing, 2014, pp. 91–134.

[36] W. Hauser, *Introduction to the Principles of Mechanics*. Addison-Wesley Publishing Company, 1965.

[37] B. Porter and R. Crossley, *Modal Control: Theory and Applications*, 0 edition. London: Taylor & Francis, 1972.

[38] K. Peleg, "Power and energy in mechanical systems," *International Journal of Mechanical Sciences*, vol. 29, no. 4, pp. 259–269, Jan. 1987.

[39] B. V. Malozyomov, N. V. Martyushev, S. N. Sorokova, E. A. Efremenkov, and M. Qi, "Mathematical Modeling of Mechanical Forces and Power Balance in Electromechanical Energy Converter," *Mathematics*, vol. 11, no. 10, p. 2394, Jan. 2023.

[40] M. R. Spiegel, *Spiegel: Applied Differential Eq.*

[41] F. Ayres, *Schaum's Outline of Theory and Problems of Differential Equations*. McGraw-Hill, 1967.

[42] W. H. Hayt, J. E. Kemmerly, S. Durbin, and S. M. Durbin, *Engineering Circuit Analysis*. 2001.

[43] W. W. Seto, *Theory and problems of mechanical vibrations:* First Edition. McGraw-Hill, 1964.

[44] W. W. Seto, *Theory and Problems of Acoustics*. .